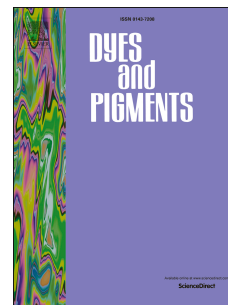


Accepted Manuscript

Rigidified Merocyanine Dyes with Different Aspect Ratios: Dichroism and Photostability

Katharina Christina Kreß, Korinna Bader, Dr. Joachim Stumpe, Prof. Dr. S.Holger Eichhorn, Prof. Dr. Sabine Laschat, Dr. Thomas Fischer



PII: S0143-7208(15)00171-0

DOI: [10.1016/j.dyepig.2015.04.041](https://doi.org/10.1016/j.dyepig.2015.04.041)

Reference: DYPI 4763

To appear in: *Dyes and Pigments*

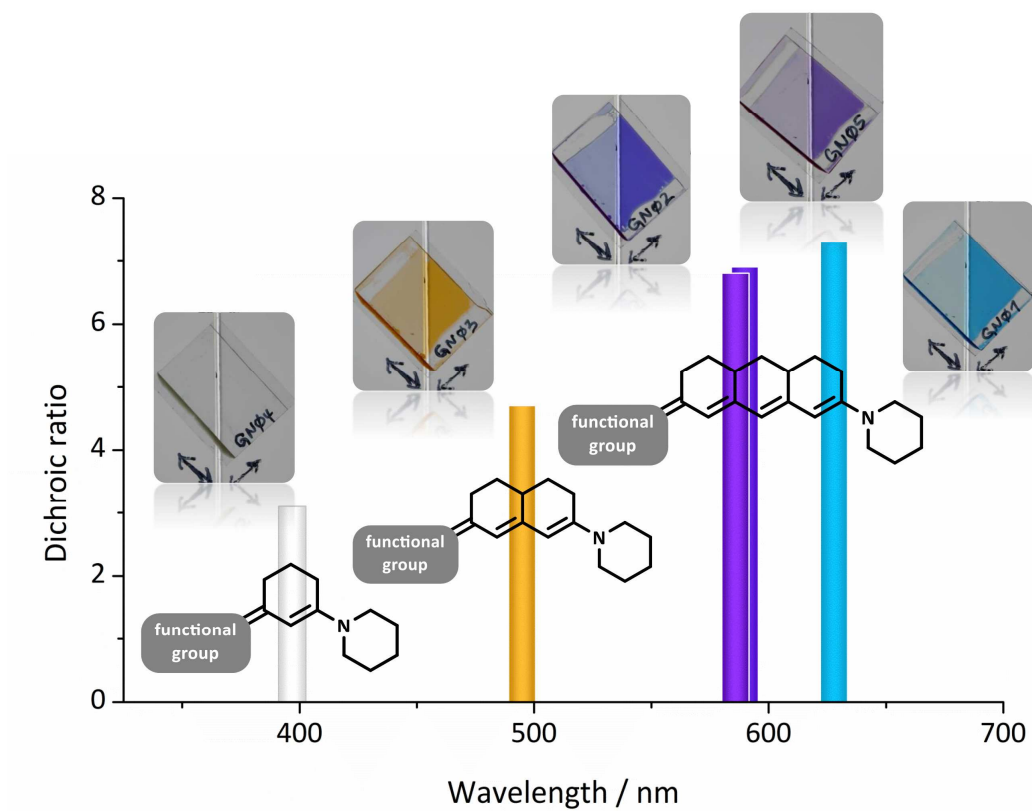
Received Date: 5 March 2015

Revised Date: 27 April 2015

Accepted Date: 29 April 2015

Please cite this article as: Kreß KC, Bader K, Stumpe J, Eichhorn SH, Laschat S, Fischer T, Rigidified Merocyanine Dyes with Different Aspect Ratios: Dichroism and Photostability, *Dyes and Pigments* (2015), doi: 10.1016/j.dyepig.2015.04.041.

This is a PDF file of an unedited manuscript that has been accepted for publication. As a service to our customers we are providing this early version of the manuscript. The manuscript will undergo copyediting, typesetting, and review of the resulting proof before it is published in its final form. Please note that during the production process errors may be discovered which could affect the content, and all legal disclaimers that apply to the journal pertain.



Rigidified Merocyanine Dyes with Different Aspect Ratios:**Dichroism and Photostability****Katharina Christina Kreß,^a Korinna Bader,^a Joachim Stumpe,^b S. Holger Eichhorn^c****Sabine Laschat^{a*} and Thomas Fischer^b**

^a K. C. Kreß, K. Bader, Prof. Dr. S. Laschat, Institut für Organische Chemie, Universität Stuttgart, Pfaffenwaldring 55, 70569 Stuttgart, (Germany), Tel: (+49) 711-68564268, E-mail: sabine.laschat@oc.uni-stuttgart.de

^b Dr. J. Stumpe, Dr. Th. Fischer, Universität Potsdam Transfer, Am Mühlenberg 11, 14476 Potsdam-Golm (Germany)

^c Prof. Dr. S. H. Eichhorn, Department of Chemistry and Biochemistry, University of Windsor, Windsor, ON, N9B 3P4 (Canada)

Highlights

- We synthesized new rigidified merocyanine dyes.
- Improvement of dichroic ratio of a guest/host system by varying the matrix.
- Increase of the photostability by alignment in a matrix.
- Proof of suitability of the dyes as thin layer polarizers and guest/host displays.

Abstract

A series of new rigidified merocyanines were investigated with regard to their optical properties as dichroic dyes. Guest/host-mixtures of the dyes were prepared using a liquid crystal and a reactive mesogen mixture. Their dichroism was studied using linearly-polarized UV/Vis-spectroscopy. A strong dependence of the dichroic ratio on the aspect ratio, the number of double bonds in the molecular structure, and on the maximum wavelength of absorption was found. A strategy to increase the aspect ratio has also been demonstrated. Additionally, the photostability was characterized using

continued irradiation with polychromatic light from a xenon source. High photostability was found in all host mixtures in the absence of oxygen by alignment in a matrix. The suitability for their application as dichroic dyes in thin layer polarizers and guest/host-displays is herein discussed.

Keywords

dichroic dye · merocyanines · aspect ratio · photostability · guest/host systems

1. Introduction

Currently, thin-film-transistor liquid crystal displays (TFT-LCDs) are the most popular flat panel displays due to their low weight, low power consumption and compact size.[1] An essential part of TFT-LCDs is the polarizing film, which is generated by stretching a polymer film containing iodine and/or dichroic dye molecules.[2] Polyvinyl alcohol/iodine polarizing films are the most widely used examples of these due to their excellent optical properties with distinct and intense absorption in the UV/Vis region.[3] However, important limitations of these polarizing films are their high sensitivity towards humidity and towards elevated temperatures due to the sublimation of iodine.[4–6]

Presently, these deficiencies are circumvented by a special lamination of the polarizing film but this packaging increases the overall thickness to several hundred microns, which makes its incorporation into the stack of functional layers within the display unfeasible. Instead, the polarizing film is typically applied on top of the display glass despite the occurrence of cross-talk by parallax that restrict fill-factor and resolution. Therefore, so-called in-cell polarizers of less than 5 microns thickness are widely investigated for a possible integration into the LC display. A promising approach based on the seminal work by Broer utilizes dichroic guest/host polarizers.[7] He reported in 1989 that selective absorption of light could be achieved by aligning a dichroic dye (guest) in an oriented, polymerisable liquid crystalline host. The low viscosity of the reactive monomeric liquid crystal

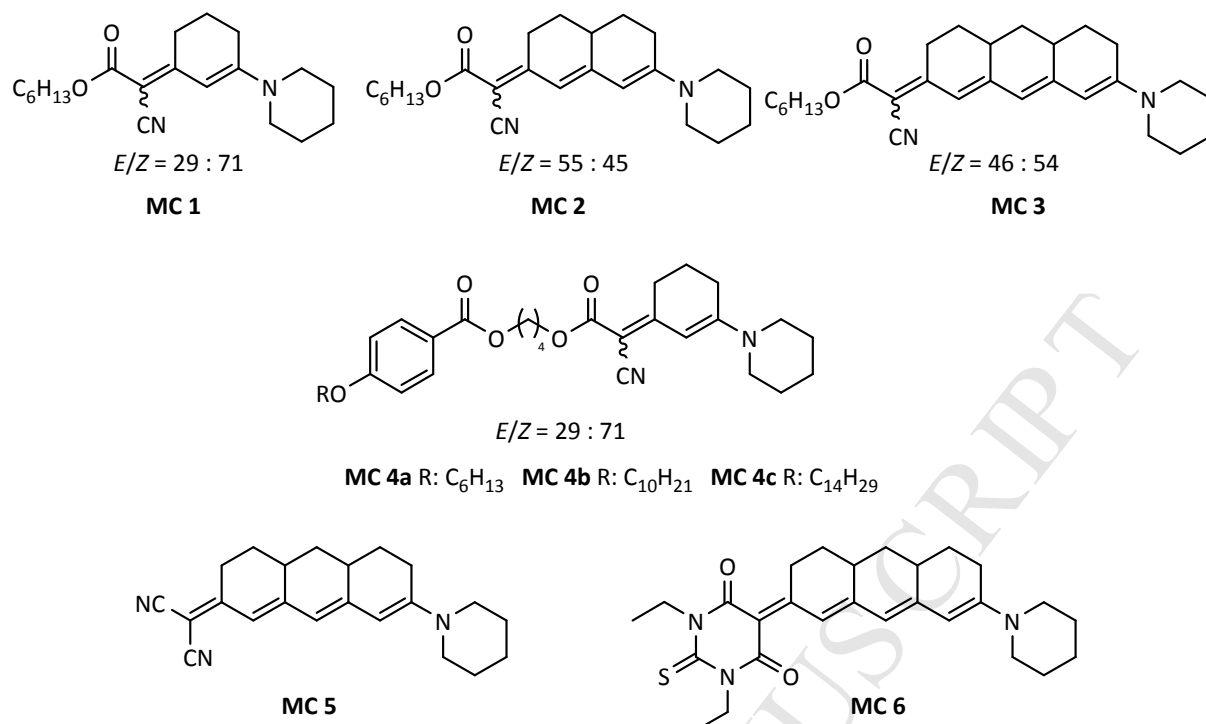
facilitates good alignment, while the *in situ* photopolymerization enables the selection of the optimum phase with highest molecular order.[8] This technology has been applied in the preparation of numerous optical devices, for example patterned retarders,[9] broadband circular polarizers,[10] wide viewing angle films,[11] and cholesteric color filters.[12] Most important properties for an application as polarizing film are a high dichroic ratio and polarizing efficiency. Both properties can be improved by increasing the molecular order of the polymeric host or preceding mesophase and by increasing the aspect ratio of the dichroic dye for a better alignment in the anisotropic host matrix. We believe the latter approach is more promising because the use of higher ordered matrices usually requires a change from nematic to smectic mesophases but the reliable fabrication of good quality smectic layers is technically much more challenging.[13]

Also, new dichroic dyes have many other potential applications such as in guest/host displays. They were invented in the late 1960s, first based on the Heilmeyer/Zanoni mode[14] and later on the White/Taylor mode.[15] The latter mode does not require additional polarizers, which promises the fabrication of simpler device geometries with lower power consumption. The lack of effective dichroic dyes and the success of devices based on the twisted nematic mode halted the development of guest/host displays, but renewed interest is currently fueled by their comparatively low cost. Potential applications include large area information displays,[16] reflective [17–19] and fluorescent displays,[20] as well as windows and tinted goggles with adjustable transparency.[21]

All these applications rely on the availability of dichroic dyes with appropriate properties. Most dichroic dyes that have been studied in displays are based on azobenzene and anthraquinone derivatives[22,23] and the objective of the work presented here is to evaluate the performance of merocyanine dyes as an alternative dichroic dye. Surprisingly few studies on the dichroism of merocyanines have been reported[13] although they have been tested for many other applications, such as in NLO devices,[24] dye sensitized solar cells,[25,26] medical peptide sensors,[27] and water

analysis,[28] because of their strong and sharp absorption bands,[29] pronounced fluorescence, solvatochromism and photochromism, and propensity to form aggregates.[30,31]

Presented herein is the first study on the dichroism of rigidified merocyanine dyes, which have a rod-like shape of adjustable aspect ratio, adjustable linear optical properties,[32] and are expected to possess high photostability. The merocyanine dyes investigated here consist of three cyanoacetates which bear different chromophoric units (trimethine **MC 1**, pentamethine **MC 2**, heptamethine **MC 3**), three cyanoacetates with tethered *p*-alkoxybenzoate units differing in their alkyl chain length (hexyl **MC 4a**, decyl **MC 4b** and tetradecyl **MC 4c**), and two other heptamethine derivatives (malononitrile **MC 5**, barbiturate **MC 6**), which carry strong acceptor groups and vary significantly in their aspect ratio (Scheme 1). To improve general solubility of the investigated compounds a benzoate unit was added to the alkyl chain in the case of derivative **MC 4**. Reported are the photostabilities of these dyes and the dichroic ratios of their mixtures with a liquid crystal (LC) and a reactive mesogen mixture (RMM) as host matrices to assess their suitability for applications in thin film polarizers. Also presented is an analysis of how different aspect ratios of the merocyanine dyes correlate with the observed dichroic ratios.



Scheme 1

2. Experimental

2.1 Materials

Synthesis. All commercial reagents were used without further purification. Solvents were dried and distilled under nitrogen prior to use and all reactions were carried out under a nitrogen atmosphere with Schlenk-type glassware. Flash chromatography was performed on silica gel, grain size 40-63 μm (Fluka).

Guest/host cells. As a LC host-material the LC-Mixture M677 of Nematel was used (a mixture of cyano- and alkoxy phenylcyclohexyl-, biphenylcyclohexyl- and bicyclohexylphenyl-derivatives). The clearing point of this mixture is 115 $^{\circ}\text{C}$. As reactive mesogen mixtures (RMM) were used RMM14 ($T_{\text{cl}} = 154$ $^{\circ}\text{C}$) and RMM34 (70 $^{\circ}\text{C}$) of Merck KGaA and a 1:1 mixture of RMM34 and ST01011 (153 $^{\circ}\text{C}$) of the Synthron GmbH.

2.2 Characterization

The following instruments were used for characterization of the compounds. NMR: *Bruker Avance* 500 (^1H , 500 MHz; ^{13}C , 125 MHz). ^1H and ^{13}C NMR spectra were referenced to TMS (Me_4Si $\delta_{\text{H}} = 0.0$ ppm, $\delta_{\text{C}} = 0.0$ ppm) as an internal standard. The following abbreviations were used: s (singlet), d (doublet), t (triplet), m (multiplet), m_{c} (centered multiplet). All spectra were recorded at room temperature. Chemical shift calculations and 2D experiments (COSY and HMBC) supported the assignments of the signals. IR: *Bruker Vector 22 FT-IR Spectrometer* with MKII golden gate single reflection Diamant ATR system. To describe the intensities following abbreviations were used: vs (very strong), s (strong), m (medium), w (weak). Elemental analyses: *Carlo Erba Strumentazione Elemental Analyzer*, Modell 1106. HRMS (ESI): *Bruker Daltonics microTOF-Q spectrometer*. Melting points: *Olympus BX50 polarizing microscope* combined with a *Linkam TP93 central controller*.

The cells were characterized by linearly polarized UV/Vis-spectroscopy. For these measurements a $\lambda 19$ spectrometer (*Perkin Elmer*) was used, which was equipped with two Glan-Taylor prisms rotated by a stepper motor. Alternatively, a polarization prism equipped diode array spectrometer TIDAS (co. J&M) was used. The dichroic ratio was calculated as $\text{DR}(\lambda) = A_{\parallel}(\lambda) / A_{\perp}(\lambda)$, whereas A_{\parallel} is the absorbance parallel and A_{\perp} perpendicular to the orientation direction. The anisotropy of fluorescence $\text{FR}(\lambda) = I_{\parallel}(\lambda) / I_{\perp}(\lambda)$ was determined in transmission geometry, whereas the excitation was carried out using linearly polarized monochromatic light with the polarization plane parallel (I_{\parallel}) and perpendicular (I_{\perp}) to the orientation direction of the sample, respectively. Remaining transmitted excitation light was absorbed by a combination of long pass filters.

2.3 Computation

Density functional theory (DFT) calculations were performed using a *Gaussian'09* software package. The geometry of the dyes was optimized using the B3LYP method with the 3-21G* basis set. The

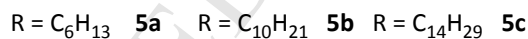
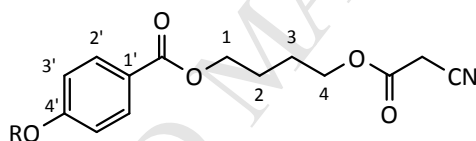
optimized structures have been classified as local minima on their respective potential energy surfaces according to their vibrational frequencies. None of the vibrational frequencies in the optimized geometries generated negative frequencies in their ground state.

2.4 Synthesis of the dyes

Compounds **2a**,^[33,34] **2b**,^[33,35] **2c**,^[33,36] **4**,^[37], **7**^[32] and **MC 6**^[24] are known in the literature (see Scheme 2). The synthesis of the molecules **MC 1**, **MC 2**, **MC 3** and **MC 5** was reported earlier.^[32] Atom numbering of compounds **5** and **MC 4** does not consequently follow the IUPAC guidelines but simplifies comparison of their NMR data.

2.4.1 The dye precursors (**5**)

General procedure for the synthesis of the dye precursors **5**



4-Alkyloxybenzoic acid (4-hexyloxy benzoic acid **2a** 650 mg, 2.93 mmol; 4-decyloxy benzoic acid **2b** 760 mg, 2.72 mmol; 4-tetradecyloxy benzoic acid **2c** 967 mg, 2.89 mmol), 4-hydroxybutyl 2-cyanoacetate (for **5a** 460 mg, 2.93 mmol; for **5b** 470 mg, 2.99 mmol; for **5c** 500 mg, 3.18 mmol), DCC (for **5a** 665 mg, 3.22 mmol) respectively EDCI (for **5b** 640 mg, 3.35 mmol; for **5c** 683 mg, 3.56 mmol), and a catalytic amount of DMAP were dissolved in dichloromethane and stirred for 48 h at room temperature. After the filtration of the insoluble components, the solvent was removed under reduced pressure. The residue was purified by flash chromatography on silica gel (petrol ether/EtOAc 5 : 1) to yield the pure products as colorless solids.

4-(2-Cyanoacetoxy) butyl 4-(hexyloxy) benzoate (5a)

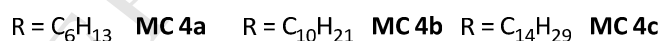
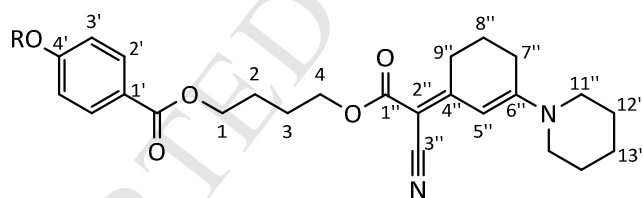
Yield: 160 mg (15%) of **5a**. Mp: 46 °C. FT-IR (ATR) (cm⁻¹): 1749 (m), 1710 (s), 1707 (s), 1606 (s), 1511 (m), 1335 (w), 1315 (w), 1276 (s), 1250 (vs), 1190 (m), 1167 (s), 1119 (m), 1102 (m), 1026 (w), 1008 (w), 848 (w), 771 (m). ¹H-NMR (CDCl₃, 500 MHz) (ppm): 0.91 (m_c, 3H, CH₃), 1.32 – 1.36 (m, 4H, CH₃CH₂CH₂), 1.47 (m, 2H, CH₂CH₂CH₂OAr), 1.80 (m_c, 2H, CH₂CH₂OAr), 1.86 (m_c, 4H, 2-H, 3-H), 3.46 (s, 2H, CH₂CN), 4.00 (t, *J* = 6.6 Hz, 2H, CH₂OAr), 4.29 (m_c, 2H, 4-H), 4.33 (m_c, 2H, 1-H), 6.91 (m_c, 2H, 3'-H), 7.97 (m_c, 2H, 2'-H). ¹³C-NMR (CDCl₃, 125 MHz) (ppm): 14.0 (CH₃), 22.6 (CH₃CH₂), 24.7 (CH₂CN), 25.2, 25.3, 25.7, 29.1, 31.5 (C-2, C-3, CH₂), 63.8 (C-1), 66.5 (C-4), 68.2 (CH₂COAr), 112.9 (CN), 114.1 (C-3') 122.2 (C-1'), 131.6 (C-2'), 162.9 (C-4'), 163.1 (C=OCH₂), 166.3 (ArC=O). HRMS (ESI) found [M+Na]⁺ 384.1782, molecular formula C₂₀H₂₇NO₅Na requires [M+Na]⁺ 384.1787. CHN: found C, 66.70; H, 7.59; N, 3.98%; molecular formula C₂₀H₂₇NO₅ requires C, 66.46; H, 7.53; N, 3.88%.

4-(2-Cyanoacetoxy) butyl 4-(decyloxy) benzoate (5b)

Yield: 130 mg (11%) of **5b**. Mp: 51 °C. FT-IR (ATR) (cm⁻¹): 2919 (m), 1733 (s), 1696 (s), 1606 (s), 1341 (m), 1278 (m), 1257 (vs), 1211 (s), 1189 (s), 1170 (vs), 1121 (m), 1105 (m), 1016 (m), 769 (s). ¹H-NMR (CDCl₃, 500 MHz) (ppm): 0.88 (m_c, 3H, CH₃), 1.21 – 1.39 (m, 12H, CH₂), 1.46 (m, 2H, CH₂CH₂CH₂OAr), 1.80 (m_c, 2H, CH₂CH₂OAr), 1.86 (m_c, 4H, 2-H, 3-H), 3.46 (s, 2H, CH₂CN), 4.00 (t, *J* = 6.6 Hz, 2H, CH₂OAr), 4.29 (m_c, 2H, 4-H), 4.33 (m_c, 2H, 1-H), 6.91 (m_c, 2H, 3'-H), 7.97 (m_c, 2H, 2'-H). ¹³C-NMR (CDCl₃, 125 MHz) (ppm): 14.1 (CH₃), 22.7 (CH₃CH₂), 24.7 (CH₂CN), 25.2, 25.3, 26.0, 29.1, 29.3, 29.4, 29.6, 31.9 (C-2, C-3, CH₂), 63.8 (C-1), 66.5 (C-4), 68.3 (CH₂OAr), 112.9 (CN), 114.1 (C-3') 122.2 (C-1'), 131.6 (C-2'), 162.9 (C-4'), 163.1 (C=OCH₂), 166.3 (ArC=O). HRMS (ESI) found [M+Na]⁺ 440.2408, molecular formula C₂₄H₃₅NO₅Na requires [M+Na]⁺ 440.2413. CHN: found C, 69.26; H, 8.40; N, 3.30%; molecular formula C₂₄H₃₅NO₅ requires C, 69.04; H, 8.45; N, 3.35%.

4-(2-Cyanoacetoxy) butyl 4-(tetradecyloxy) benzoate (5c)

Yield: 160 mg (12%) of **5c**. Mp: 61 °C. FT-IR (ATR) (cm^{-1}): 2957 (m), 2915 (vs), 2850 (s), 1737 (s), 1712 (vs), 1607 (m), 1472 (m), 1344 (m), 1321 (w), 1282 (m), 1254 (s), 1219 (w), 1189 (m), 1171 (m), 769 (m). $^1\text{H-NMR}$ (CDCl_3 , 500 MHz) (ppm): 0.88 (m_c , 3H, CH_3), 1.22 – 1.39 (m, 20H, CH_2), 1.46 (m, 2H, $\text{CH}_2\text{CH}_2\text{CH}_2\text{OAr}$), 1.80 (m_c , 2H, $\text{CH}_2\text{CH}_2\text{OAr}$), 1.86 (m_c , 4H, 2-H, 3-H), 3.46 (s, 2H, CH_2CN), 4.00 (t, $J = 6.6$ Hz, 2H, CH_2OAr), 4.29 (m_c , 2H, 4-H), 4.33 (m_c , 2H, 1-H), 6.91 (m_c , 2H, 3'-H), 7.97 (m_c , 2H, 2'-H). $^{13}\text{C-NMR}$ (CDCl_3 , 125 MHz) (ppm): 14.1 (CH_3), 22.7 (CH_3CH_2), 24.7 (CH_2CN), 25.2, 25.3, 26.0, 29.1, 29.4, 29.57, 29.61, 29.67, 29.69, 29.70, 31.9 (C-2, C-3, CH_2), 63.8 (C-1), 66.5 (C-4), 68.3 (CH_2OAr), 114.1 (C-3'), 122.2 (C-1'), 131.6 (C-2'), 162.9 (C-4'), 163.1 ($\text{C}=\text{OCH}_2$), 166.4 ($\text{ArC}=\text{O}$). HRMS (ESI) found $[\text{M}+\text{Na}]^+$ 496.3034, molecular formula $\text{C}_{28}\text{H}_{43}\text{NO}_5\text{Na}$ requires $[\text{M}+\text{Na}]^+$ 496.3039. CHN: found C, 70.95; H, 9.16; N, 2.94%; molecular formula $\text{C}_{28}\text{H}_{43}\text{NO}_5$ requires C, 71.00; H, 9.15; N, 2.96%.

2.4.2 The benzoate dyes (MC 4)**General procedure for the Knoevenagel condensation[38,39]**

To an ice-cooled solution of trimethyloxonium tetrafluoroborate (for **MC 4a** 259 mg, 1.75 mmol; for **MC 4b** 135 mg, 0.91 mmol; for **MC 4c** 155 mg, 1.05 mmol) in absolute dichloromethane was added the carbonyl compound **7** (for **MC 4a** 179 mg, 1.00 mmol; for **MC 4b** 93 mg, 0.52 mmol; for **MC 4c** 107 mg, 0.60 mmol) at 0 °C and the resulting mixture was warmed to room temperature. After stirring for 12 h the oxonium salt was precipitated by addition of *n*-pentane. In a second flask, the acceptor moiety (**5a** 180 mg, 0.50 mmol; for **5b** 110 mg, 0.26 mmol; for **5c** 142 mg, 0.30 mmol) was treated with DBU (for **MC 4a** 0.13 mL, 0.90 mmol; for **MC 4b** 0.07 mL, 0.47 mmol; for **MC 4c** 0.08 mL,

0.54 mmol) and the mixture was stirred for 45 min at room temperature. The above described oxonium salt was added and the reaction mixture was heated to 80 °C for 2 h and subsequently stirred for further 2 h at room temperature. The mixture was diluted with dichloromethane and washed with 1 N hydrochloric acid. The aqueous layer was separated, extracted with dichloromethane and the combined organic layers were washed with brine, dried over anhydrous magnesium sulfate, filtered and the solvent was removed under reduced pressure. The residue was purified by flash chromatography on silica gel (petrol ether/EtOAc 2 : 1) to yield the yellow solid products as inseparable mixtures of double bond isomers.

4-(2-Cyano-2-(3-(piperidin-1-yl) cyclohex-2-en-1-ylidene) acetoxy) butyl-4-(hexyloxy)-benzoate (MC 4a)

Yield: 105 mg (40%) of **MC 4a** (isomeric ratio *E/Z* = 29 : 71 according to ¹H-NMR). Mp: 61 °C. FT-IR (ATR) (cm⁻¹): 2957 (m), 2915 (vs), 2850 (s), 1737 (s), 1712 (vs), 1607 (m), 1472 (m), 1344 (m), 1321 (w), 1282 (m), 1254 (s), 1219 (w), 1189 (m), 1171 (m), 769 (m). ¹H-NMR (CDCl₃, 500 MHz) (ppm, *E*-isomer signals labeled with *): 0.90 (m_c, 3H, CH₃), 1.32 – 1.35 (m, 4H, CH₃CH₂CH₂), 1.45 – 1.47 (m, 2H, CH₂CH₂CH₂OAr), 1.62 – 1.68 (m, 4H, 12''-H), 1.68 – 1.74 (m, 2H, 13''-H), 1.79 (m_c, 2H, CH₂CH₂OAr), 1.82 – 1.95 (m, 6H, 2-H, 3-H, 8''-H), 2.40 (m_c, 0.6H, 7''-H*), 2.44 (m_c, 1.4H, 7''-H), 2.66 (m_c, 1.4H, 9''-H), 3.05 (m_c, 0.6H, 9''-H*), 3.45 – 3.50 (m, 1.4H, 11''-H*), 3.50 – 3.55 (m, 2.6H, 11''-H), 4.00 (t, *J* = 6.6 Hz, 2H, CH₂OAr), 4.17 – 4.23 (m, 2H, 4-H), 4.32 (m_c, 2H, 1-H), 6.03 (s, 0.3H, 5''-H*), 6.89 (m_c, 2H, 3'-H), 7.41 (s, 0.7H, 5''-H), 7.98 (m_c, 2H, 2'-H). ¹³C-NMR (CDCl₃, 125 MHz) (ppm, *E*-isomer signals labeled with *): 14.0 (CH₃), 21.8 (C-8''), 21.9 (C-8''*), 22.6 (C-10'), 24.2, 25.7 (C-12'', C-13''), 25.5, 25.68, 25.74, 31.6 (C-2, C-3, CH₂), 26.8 (C-9''*), 27.2 (C-7''*), 27.4 (C-7''), 29.1 (CH₂CH₂OAr) 29.7 (C-9''), 48.0 (C-11''*), 48.3 (C-11''), 63.3 (C-1), 64.3 (C-4), 68.2 (CH₂OAr), 81.1 (C-4''), 97.6 (C-5''), 98.3 (C-5''*), 114.0 (C-3'), 122.6 (C-1'), 131.6 (C-2'), 162.7 (C-6''), 162.9 (C-4'), 166.2 (C-1''), 166.5 (ArC=O), 167.8 (C-3''), 170.6 (C-2''). HRMS (ESI) found [M+Na]⁺ 545.2986, molecular formula C₃₁H₄₂N₂O₅Na

requires $[M+Na]^+$ 545.2991. CHN: found C, 71.23; H, 8.09; N, 5.20%; molecular formula $C_{31}H_{42}N_2O_5$ requires C, 71.24; H, 8.10; N, 5.36%.

4-(2-Cyano-2-(3-(piperidin-1-yl)cyclohex-2-en-1-ylidene)acetoxy) butyl-4-(decyloxy)-benzoate (MC 4b)

Yield: 56 mg (39%) of **MC 4b** (isomeric ratio $E/Z = 29 : 71$ according to 1H -NMR). Mp: 72 °C. FT-IR (ATR) (cm^{-1}): 1538 (m), 1503 (s), 1251 (s), 1224 (s), 1195 (vs), 1166 (s), 1135 (m), 1099 (s), 1074 (m), 1019 (m), 997 (m), 977 (w), 845 (w), 769 (m), 729 (s). 1H -NMR ($CDCl_3$, 500 MHz) (ppm, E -isomer signals labeled with 0.88 (m_c , 3H, CH_3), 1.21 – 1.39 (m, 12H, CH_2), 1.45 – 1.47 (m, 2H, $CH_2CH_2CH_2OAr$), 1.61 – 1.68 (m, 4H, $12''-H$), 1.68 - 1.74 (m, 6H, $13''-H$), 1.79 (m_c , 2H, CH_2CH_2OAr), 1.82 – 1.95 (m, 6H, 2-H, 3-H, $8''-H$), 2.41 (m_c , 0.6H, $7''-H^*$), 2.45 (m_c , 1.4H, $7''-H$), 2.66 (m_c , 1.4H, $9''-H$), 3.05 (m_c , 0.6H, $9''-H^*$), 3.45 – 3.50 (m, 1.4H, $11''-H^*$), 3.50 – 3.55 (m, 2.6H, $11''-H$), 4.00 (t, $J = 6.6$ Hz, 2H, CH_2OAr), 4.17 – 4.23 (m, 2H, 4-H), 4.32 (m_c , 2H, 1-H), 6.03 (s, 0.3H, $5''-H^*$), 6.89 (m_c , 2H, $3'-H$), 7.41 (s, 0.7H, $5''-H$), 7.98 (m_c , 2H, $2'-H$). ^{13}C -NMR ($CDCl_3$, 125 MHz) (ppm, E -isomer signals labeled with *): 14.1 (CH_3), 21.8 (C-8''), 21.9 (C-8''*), 22.7 (CH_3CH_2), 24.2, 25.7 (C-12'', C-13''), 25.4, 25.5, 25.68, 25.3, 26.0, 29.4, 29.5, 31.9 (C-2, C-3, CH_2), 26.8 (C-9''*), 27.1 (C-7''*), 27.4 (C-7''), 29.1 (CH_2CH_2OAr), 29.7 (C-9''), 48.0 (C-11''*), 48.3 (C-11''), 63.2 (C-1), 64.2 (C-4), 68.2 (CH_2OAr), 80.8 (C-4''), 97.6 (C-5''), 98.3 (C-5''*), 114.0 (C-3'), 122.5 (C-1'), 131.6 (C-2'), 162.7 (C-6''), 162.9 (C-4'), 166.2 (C-1''), 166.4 (ArC=O), 167.7 (C-3''), 170.6 (C-2''). HRMS (ESI) found $[M+Na]^+$ 601.3612, molecular formula $C_{35}H_{50}N_2O_5Na$ requires $[M+Na]^+$ 601.3617. CHN: found C, 72.43; H, 8.73; N, 4.71%; molecular formula $C_{35}H_{50}N_2O_5$ requires C, 72.63; H, 8.71; N, 4.84%.

4-(2-Cyano-2-(3-(piperidin-1-yl)cyclohex-2-en-1-ylidene)acetoxy) butyl-4-(tetradecyloxy)-benzoate (MC 4c)

Yield: 108 mg (57%) of **MC 4c** (isomeric ratio $E/Z = 29 : 71$ according to 1H -NMR). Mp: 63 °C. FT-IR (ATR) (cm^{-1}): 1538 (m), 1504 (s), 1444 (w), 1331 (w), 1277 (w), 1253 (s), 1226 (s), 1196 (vs), 1167 (s), 1100 (m), 1019 (w), 906 (s), 846 (w), 770 (w), 727 (vs), 647 (w). 1H -NMR ($CDCl_3$, 500 MHz) (ppm, E -

isomer signals labeled with *): 0.88 (m_c, 3H, CH₃), 1.21 – 1.39 (m, 20H, CH₂), 1.44 – 1.46 (m, 2H, CH₂CH₂CH₂OAr), 1.61 – 1.68 (m, 4H, 12''-H), 1.68 - 1.74 (m, 2H, 13''-H), 1.79 (m_c, 2H, CH₂CH₂OAr), 1.82 – 1.95 (m, 6H, 2-H, 3-H, 8''-H), 2.41 (m_c, 0.6H, 7''-H*), 2.45 (m_c, 1.4H, 7''-H), 2.65 (m_c, 1.4H, 9''-H), 3.05 (m_c, 0.6H, 9''-H*), 3.45 – 3.50 (m, 1.4H, 11''-H*), 3.50 – 3.55 (m, 2.6H, 11''-H), 4.00 (t, *J* = 6.6 Hz, 2H, CH₂OAr), 4.17 – 4.23 (m, 2H, 4-H), 4.32 (m_c, 2H, 1-H), 6.02 (s, 0.3H, 5''-H*), 6.89 (m_c, 2H, 3'-H), 7.41 (s, 0.7H, 5''-H), 7.97 (m_c, 2H, 2'-H). ¹³C-NMR (CDCl₃, 125 MHz) (ppm, *E*-isomer signals labeled with *): 14.1 (CH₃), 21.7 (C-8''), 21.9 (C-8''*), 22.7 (CH₃CH₂), 24.1, 25.7 (C-12'', C-13''), 25.4, 25.5, 25.68, 26.0, 29.3, 29.54, 29.57, 92.64, 29.66, 31.9 (C-2, C-3, CH₂), 26.8 (C-9''*), 27.1 (C-7''*), 27.4 (C-7''), 29.1 (CH₂CH₂OAr) 29.7 (C-9''), 48.0 (C-11''*), 48.3 (C-11''), 63.2 (C-1), 64.2 (C-4), 68.2 (CH₂OAr), 80.8 (C-4''), 97.6 (C-5''), 98.2 (C-5''*), 114.0 (C-3'), 122.5 (C-1'), 131.6 (C-2'), 162.6 (C-6''), 162.9 (C-4'), 166.1 (C-1''), 166.4 (ArC=O), 167.7 (C-3''), 170.6 (C-2''). HRMS (ESI) found [M+Na]⁺ 657.4238, molecular formula C₃₉H₅₈N₂O₅Na requires [M+Na]⁺ 657.4243. CHN: found C, 73.61; H, 9.22; N, 4.25%; molecular formula C₃₉H₅₈N₂O₅ requires C, 73.78; H, 9.21; N, 4.41%.

2.5 Preparation of the guest/host samples

Preparation of the dye guest/host mixtures. An appropriate amount (0.5 to 1.3 wt%) of the dye material was added to the host material and dissolved in a mass equivalent of dry chloroform. In the case of the 1:1 mixture RMM34/ST01011 a 1 wt% of the photo-initiator Irg 1700 and 0.1 wt% of thermal inhibitors phenoxazin and 4-methoxyphenol were added while preparing these mixtures. The solution was stirred for 1 h and then the solvent was allowed to evaporate at room temperature in order to avoid unwanted thermal polymerization (in the case of reactive mesogen mixtures). Subsequently, the remaining solvent was evaporated in vacuum until the remaining mass was that of the mixture components. This procedure ensures the formation of homogenous mixtures.

Liquid crystal guest/host mixture cells. The cells used in this study were purchased from company Instec. Cells with a gap of 8 μm were filled with the LC guest/host-mixtures by capillary forces at

140 °C. After complete filling the cells were allowed to cool down to room temperature slowly. Subsequently, the cells were sealed using an epoxy resin. This was done for the LC guest/host-mixtures of the compounds **MC 1**, **MC 2**, **MC 3**, **MC 4a-c**, **MC 5** and **MC 6**. In all cases a uniform macro domain was observed between crossed polarizers.

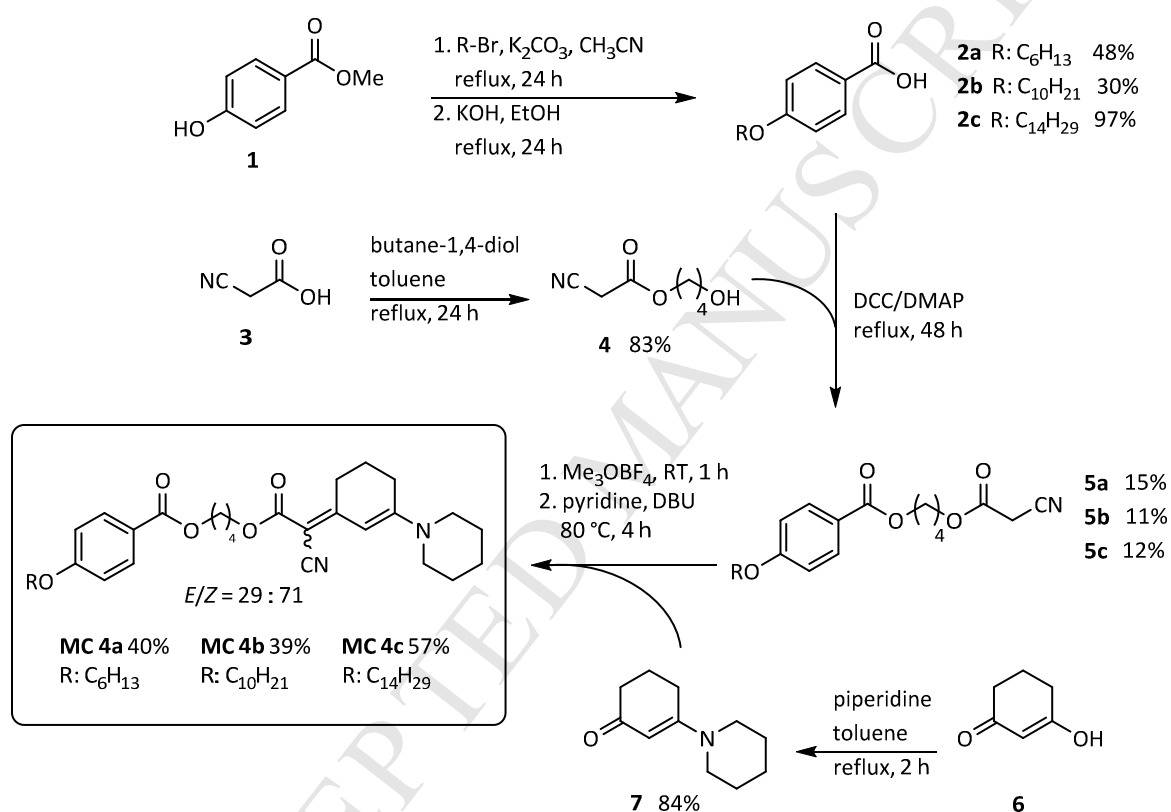
Reactive mesogen guest/host mixture cells. For the characterization of the dichroism of reactive mesogen g/h-mixtures cells with a gap of 10 μm were prepared. As material for the aligning layers the polyimide SE-130 (Nissan/SunEver) was spin-coated on glass substrates. After the coating procedure the layers were dried at 80 °C for 5 min and subsequently backed at 180 °C for 1 h to achieve full imidization. These substrates were rubbed using a machine of company Beamco. The substrates were fixed to form a cell with anti-parallel orientation. The gap of about 10 μm was ensured using spacer particles of the same dimension dispersed in the epoxy resin lines at the long edges of the substrates. The filling of the cells were carried out by capillary forces at 110 °C. The samples were heated shortly to 160 °C and then slowly cooled down to room temperature. The photo induced cross-linking was done by irradiation with a fluorescent tube emitting at 365 nm (Philips PL-S / 10 UV-A). The used dose was app. 250 mJ/cm^2 . At this dose a sufficient cross-linking is reached to fix the well oriented domain. Subsequently, the cells were sealed using an epoxy resin.

Photostability in solution. The used set-up was built up using a diode array spectrometer (XDAP, co. Polytech) and a xenon arc lamp (XBO 75). The infrared component of the light was removed by a water cuvette. For the irradiation procedure the light was directed to the sample in normal incidence by using a motorized mirror. Before the UV/Vis-measurements the mirror was tilted out computer controlled and tilted in again after. The intensity of the polychromatic light of the xenon source was measured with a LM2 detector and a Fieldmaster powermeter (both of co. Coherent). The measured value was correlated to the maximum of the intensity distribution at 475 nm. The power density was app. 150 mW/cm^2 . The concentration of the different merocyanine dyes in the solution was adjusted

to be app. of absorbance 1 using acetonitrile as solvent. During irradiation and measurement the solution was stirred with a magnetic micro bar in order to ensure a homogenous concentrated solution.

3. Results and discussion

3.1 Synthesis



Scheme 2

As shown in Scheme 2, methyl 4-hydroxybenzoate **1** was alkylated using alkyl bromides in the presence of K_2CO_3 in CH_3CN and subsequently deprotected with KOH in ethanol giving the free acids **2a-c** in good yields over two steps.[40,41] The ester **4** was obtained according to Parkers procedure from 2-cyanoacetic acid **3** and butane-1,4-diol.[42] Following Steglich esterification[43] the esters **5a-c** were synthesized in moderate yields, hampered by incomplete conversion. In order to obtain dye precursor β -enamino ketone **7** the method from Greenhill[44] was applied by refluxing

3-hydroxycyclohexenone **6** with piperidine in toluene under Dean–Stark conditions for 5 h, which yielded the product **7** in 84%. For the Knoevenagel condensation, the ketone derivative **7** was activated with $\text{Me}_3\text{O}^+\text{BF}_4^-$ according to the method by Kreß[32] and subsequently treated with the cyanoacetate derivative in the presence of DBU in pyridine at 80 °C. The yellow solid dyes **MC 4a-c** were obtained as inseparable *E/Z*-isomers (29 : 71) in yields between 39-57%. The synthesis of compounds **MC 1**, **MC 2**, **MC 3**, **MC 5** and **MC 6** was reported earlier.[32,38]

3.2 Calculated aspect ratios

To quantify the shape anisotropy of the rod-shaped dyes, a crucial factor for their dichroic properties, the aspect ratios (*AR*) were calculated based on their minimum energy conformations in the gas phase (DFT, B3LYP 3-21G*). **Error! Reference source not found.** shows the optimized structure of *E*-**MC 4a** (all structures are shown in the supporting information). Calculations were carried out based on the assumption that the whole molecule rotates around its long axis. W_{core} was defined as the width of the chromophoric unit and L_{core} as the length of the chromophoric unit including the piperidine moiety. The values W_{core} and L_{core} were determined from the calculated optimized geometries. Following a reported procedure L_{chain} can be estimated based on the assumption that the core occupies a cylindrical volume (free rotation about the long axis in the LC state) and that the side chains must occupy a cylindrical volume of the same diameter.[45] The required value of V_{chain} was calculated using reported increment volume values for aliphatic chains in the liquid state.[46–48] Averaged AR_{ϕ} values are reported for dyes that consist of mixtures of *E* and *Z* isomers by taking into account their measured *E/Z*-ratios.

A comparison of the AR_{ϕ} values in Table 1 clearly shows that the extension of alkyl chains increases the ARs of the benzoate derivatives **MC 4** much more (40%) than for the cyanoacetates **MC 1-3**

(24%). Malodinitrile **MC 5** and thiobarbiturate **MC 6**, being devoid of the hexylester chain, show comparably smaller aspect ratios of 2.0 and 1.9 respectively.

3.3 Dichroism of the different merocyanines

3.3.1 Dichroism in a liquid crystalline matrix

For applications of dichroic dyes in guest/host displays or functional dichroic layers, the miscibility of the dye with the LC host is of importance. The commercially available LC mixture M677 with a relatively high clearing point of 115 °C was chosen as a benchmark host for the compatibility studies. All merocyanines studied here showed a good solubility in the host over a concentration range of 0.5 – 1.3 wt% except for **MC 5** that started to separate upon cooling below 80 °C. The dichroism of the anisotropic solutions was studied by linear polarized UV/Vis-spectroscopy utilizing thin film cells which displayed homogeneous macro domains (except for **MC 5**) (see Table 2).

Figure 2 shows the absorption spectra of compound **MC 2** and **MC 6** for parallel and perpendicular polarized light revealing a distinct dichroism (all absorption spectra are shown in the supporting information). Similar results were obtained for the other merocyanine derivatives. The dichroic ratios DR , i.e. the ratio of the absorbance at maxima parallel and perpendicular to the orientation direction A_{\parallel}/A_{\perp} are summarized in Table 2 together with the aspect ratio.

Due to the poor reproducibility caused by partial crystallization, the DR values of compound **MC 5** were not considered. Presumably, the host mixture M677 is not suitable for a highly polar guest such as the malononitrile **MC 5**. As shown in Table 2, the dichroic ratio grows with the increasing length of the conjugated π -system and the wavelengths of the absorption maxima. This is observed most prominently within the homologous series of mono-, bi- and tricyclic merocyanines **MC 1**, **MC 2** and **MC 3** as illustrated in Figure 3a. Both the increased number of double bonds and thus the improved delocalization of the π -system, as well as increasing the strengths of the donor/acceptor moieties

lead to a higher polarizability and dipole moment resulting in an increased dichroic ratio. Furthermore, the dichroic ratio appears to directly depend on the aspect ratio (Figure 3b), which means an increase in shape anisotropy of the chromophoric system significantly enhances its alignment within the anisotropic host and, consequently, increases the measured dichroism.

In order to study the two parameters separately, merocyanines **MC 4a-c** were chosen, where the chromophoric unit was kept constant, while the aspect ratio increased from 5.1 (for **MC 4a**) to 8.1 (for **MC 4c**). For all three compounds the same dichroic ratio of 2.5 was found, which is somewhat smaller as compared to the related merocyanine **MC 1** ($DR = 2.9$). This is probably due to the fact that the longitudinal molecular axis of **MC 4a-c** is no longer parallel to the transition dipole moment as it was in the case of **MC 1**. Although with an increasing shape anisotropy of the dye molecule a much better degree of order within the LC host should be expected. The macroscopic dichroism is driven by the dichroism of the chromophoric system, often characterized as the degree of order of the transition moment.[49] The macroscopic dichroism is a product of the substitution pattern, lengths and anisotropy of the π -system, the angle between the longitudinal molecular axis and the direction of the transition dipole moment of the chromophore, the geometric aspect ratio of the dye molecule, and the order of the anisotropic host matrix.[49–51]

Our calculations reveal that the increased lengths of the benzoate units in **MC 4a-c** do indeed lead to an increase of the aspect ratio, which was found beneficial for the solubility in the LC host. However, in order to improve the dichroic ratio, the mesogenic (or mesogen-like) unit of the chromophore, such as *p*-alkoxybenzoate, should not change the orientation of the longitudinal molecular axis, as compared to the non-mesogenic counterpart **MC 1**. By maintaining a subtle balance between these different parameters an improvement of the dichroic ratio should be achieved.

3.3.2 Dichroism in a RMM matrix

To investigate the suitability of the merocyanines for in-cell polarizers or anisotropic emitters a mixture of the merocyanine dye **MC 3** with the commercially available reactive mesogen host RMM34 (0.6 wt%) was filled into 2 μm thin-film cells, annealed, and photo-crosslinked via acrylate groups at room temperature to stabilize the nematic domains. The homogeneous appearance of the thin-film cells indicates a good miscibility of the dye in the host matrix. A strong dichroism of tricyclic cyanoacetate **MC 3** was detected in the linear polarized UV/Vis spectrum accompanied by a high anisotropy of the fluorescence intensity (Figure 4).

The fluorescence spectrum of compound **MC 3** obtained by excitation with linear polarized light at 594 nm parallel and perpendicular to the orientation direction displayed a strong emission at 644 nm with a Stokes shift of 47 nm and a pronounced fluorescence anisotropy $I_{\parallel}/I_{\perp} = 6.0$. These results indicate that the emission is not disturbed by additional interactions causing depolarization. However, the experimentally observed dichroic ratio ($DR = 6.0$) of the **MC 3**/RMM34 mixture is significantly smaller than the value obtained for the **MC 3**/M677 mixture ($DR = 7.9$). This might be due to the lower clearing point of the reactive mesogen mixture RMM34 ($T_{cl} = 70\text{ }^{\circ}\text{C}$) as compared to the clearing transition of the LC mixture M677 at $T_{cl} = 115\text{ }^{\circ}\text{C}$. This means the host RMM34 is less ordered at room temperature than the LC mixture M677 expressed by the higher reduced temperature (RT/T_{cl}).^[52] In order to increase the clearing temperature of the reactive mesogen mixture, a mixture of RMM34 and the reactive mesogen ST01011 (1 : 1) with a clearing point of 153 $^{\circ}\text{C}$ was used for all subsequent experiments.

The values of the dichroic ratio of the various merocyanines using this particular host are summarized in Figure 5 together with photos of the thin-film cells. The photos were taken using linear polarized light, left part perpendicular and right parallel to the orientation direction, visualizing the extent of dichroism and presence of homogeneous macro domains. The guest/host-systems

containing the reactive mesogen mixture display a similar trend concerning the dichroism, as was found for the LC host. Thus, DR values increase with increasing wavelengths of the absorption maxima due to the increase of the extension and delocalization of the π -system. Tricyclic thiobarbiturate **MC 6** possessing the most bathochromically shifted absorption ($\lambda_{\max} = 628$ nm) shows the largest dichroic ratio ($DR = 7.3$). We anticipated that a further improvement of the DR value should be possible by employing a more highly ordered matrix. In a proof-of-principle experiment the reactive mesogen mixture RMM14 possessing an additional weak smectic A phase was used as a host and combined with tricyclic malodinitrile **MC 5**. Gratifyingly, over the whole absorption range improved dichroism was found and the DR value at $\lambda_{\max} = 644$ nm increased to 12.6, while fluorescence measurements revealed a fluorescence anisotropy $I_{\parallel}/I_{\perp} = 9.7$ ($\lambda_{\text{exc}} = 622$ nm). These values are in the range of best reported results for nematic hosts.[18,20] This increase of the dichroic ratio using higher ordered hosts lets expect that the tricyclic merocyanines would give in smectic B hosts a strong dichroism suitable for high performance thin-film polarizers comparable to the best results in the literature.[8]

3.4 Photostability

3.4.1 Photostability in solution

Error! Reference source not found. shows the spectra of **MC 3** in CH_3CN upon irradiation with a xenon lamp. Significant photodegradation was observed upon ongoing irradiation, while simultaneously the absorption in the UV-region increased.

A similar behavior was found for all investigated merocyanine derivatives, although **MC 1** was the most stable of this series. This might be due to the fact that its absorption maximum ($\lambda_{\max} = 397$ nm) does not coincide with the intensity maximum of the polychromatic light source. Thus, the amount of absorbed light is reduced in comparison to the merocyanines with a bathochromically shifted

absorption maximum, e.g. **MC 3** ($\lambda_{\max} = 590 \text{ nm}$). In order to reduce the influence of the intensity distribution the xenon light dose was corrected by applying wavelength dependent factors taken from the literature.[53] The correlation between the normalized absorbance at the absorption maxima and the corrected light dose for the various dyes is shown in Figure 7.

In general, the photostability decreased with increasing number of double bonds in the chromophoric system (e.g. **MC 1** > **MC 2** > **MC 3**). A possible reason for this partial photodegradation might be photooxidation, as was previously described in the literature for unbranched merocyanines.[54] In this work especially the merocyanine MC540 was investigated as a potential photochemotherapeutic agent and a photooxidation mechanism was discussed.[55–57] In order to evaluate this mechanism further for our stability experiments, the cuvette was flushed with dry N_2 for 30 min before use and subsequently sealed in order to attempt to significantly reduce the presence of oxygen during future measurements. **Error! Reference source not found.** shows the absorption behavior with untreated (oxygen-containing) and N_2 -treated cuvettes. After initial photodegradation in the N_2 -treated solution a steady-state was reached without further decrease of the absorbance upon prolonged irradiation.

This experiment might prove that the dominating mechanism of the photodegradation is indeed caused by a photooxidation. The photodegradation at the beginning of the experiment may be due to remaining traces of dissolved oxygen in the system and similar results have been found in literature.[58]

3.4.2 Photostability in a LC and in a RMM matrix

Regarding the suitability of the merocyanines for guest/host-displays their photostability in the LC and RMM thin-film cells was investigated. The first experiments were performed with the $10 \mu\text{m}$ thin-film cells under similar conditions as previously described for the solution experiments. **Error!**

Reference source not found. shows the spectra of bicyclic cyanoacetate **MC 2** as a function of irradiation time. In contrast to the solution spectra (Figure 6), the absorption bands did not change except for the appearance of a weak band at ca. 550 nm, which develops with increasing irradiation time, presumably due to a photo-induced process generated product. A similar phenomenon was observed for **MC 3** and **MC 6**, where photoinduced products always appeared with a bathochromic shift of 50 nm relative to their absorption maxima. **Error! Reference source not found.** shows the normalized extinctions at the absorption maximum as a function of the irradiation time.

For all studied merocyanines the absorbance remains almost constant irrespective of the irradiation time. The slight increase of the curves of **MC 3** and **MC 6** might be caused the presence of trace amounts of photoinduced byproducts. All investigated merocyanines showed a much higher photostability upon irradiation in the LC matrix as compared to the solution. This could be reasoned to the lower solubility and diffusion rate of oxygen in the LC mixture in comparison.

In order to investigate the photostability of the RMM matrix, thin-film cells containing 0.6wt% of **MC 3** in RMM34 were irradiated in a similar fashion and the time-dependent fluorescence intensity parallel to the orientation alignment of the cell was studied (Figure 11). Pleasingly, the emission intensity remained almost constant even after 30 min of irradiation time ($\lambda_{\text{exc}} = 590 \text{ nm}$) and no degradation could be detected. Similar results were observed for all subsequently studied merocyanines, demonstrating the high photochemical stability of the reactive mesogen mixture as a host.

Conclusion

In this study we have investigated a series of known and new merocyanines, differing in their number of rings, donor and acceptor moieties and degrees of functionalization of the donor unit, with regard to their dichroism and photostability in different matrices. UV/Vis-spectroscopy with linearly-polarized light revealed that the dichroic ratio increases with increasing wavelengths of the

absorption maxima irrespective of the host. In other words, upon comparison of the LC-mixture MM67 with the reactive mesogen mixture RMM34/ST01011 (1 : 1) as hosts, similar *DR* values were obtained for a certain chromophoric guest. The highest dichroic ratios of up to 7.9 were obtained for tricyclic merocyanines **MC 3**, **MC 5** and **MC 6**. By using a reactive mesogen mixture (RMM14) with a higher degree of order, the dichroic ratio could be further improved to 12.6 for **MC 6**. Furthermore, fluorescence anisotropy correlates well with the dichroism, e.g. $I_{\parallel}/I_{\perp} = 9.7$ ($\lambda_{\text{exc}} = 622$ nm) for **MC 6**.

Although attachment of mesogen-like substituents to the donor moiety increased the aspect ratio considerably according to DFT calculations, the extent of π -delocalization, together with the bathochromic shift of the absorption maximum, contributes to the dichroism to a much larger extent. The attachment of aspect ratio increasing substituent must not change the coincidence of transition moment and long molecular axis.

In order to assess the photostability of the merocyanines, time-dependent UV/Vis- and fluorescence spectra were performed in solution, in an LC-matrix, and in a reactive mesogen matrix. While experiments in solution revealed considerable photodegradation, which could be partially suppressed by flushing the solution with N_2 , experiments conducted in the LC and RMM demonstrated a considerably high photostability of the investigated dyes. In particular, the use of the reactive mesogen matrix as the host yielded almost constant fluorescence intensities even after prolonged irradiation times. Thus, we have shown that the tricyclic merocyanines **MC 3**, **MC 5** and **MC 6** are well suited for applications as dichroic dyes in thin-film polarizers and guest/host displays.

Acknowledgements

General financial support by the Carl-Zeiss-Stiftung (fellowship for K.C.K.), the International Max-Planck-Research-School on Advanced Materials (fellowship for K.C.K.), the Fonds der Chemischen Industrie, the Ministerium für Wissenschaft, Forschung und Kunst des Landes Baden-Württemberg

and the GDCh (travel grant for K.C.K.) is gratefully acknowledged. Thanks also goes to Dr. U. Lawrentz for the synthesis of **MC 6** and Dr. Johannes for supplying us with the dye as well as to Mr. S. Beardsworth for proof reading the manuscript.

Literature

- [1] Ma J, Ye X, Jin B. Structure and application of polarizer film for thin-film-transistor liquid crystal displays. *Displays* 2011;32:49–57. doi:10.1016/j.displa.2010.12.006.
- [2] Land EH. Some Aspects of the Development of Sheet Polarizers. *J Opt Soc Am* 1951;41:957–62. doi:10.1364/JOSA.41.000957.
- [3] Chang JB, Hwang JH, Park JS, Kim JP. The effect of dye structure on the dyeing and optical properties of dichroic dyes for PVA polarizing film. *Dyes Pigments* 2011;88:366–71. doi:10.1016/j.dyepig.2010.08.007.
- [4] Shin EJ, Lyoo WS, Lee YH. Making polyvinyl alcohol films iodinated at solution state before casting and its application. *J Appl Polym Sci* 2008;109:1143–9. doi:10.1002/app.28181.
- [5] Shin EJ, Lee YH, Choi SC. Study on the structure and processibility of the iodinated poly(vinyl alcohol). I. Thermal analyses of iodinated poly(vinyl alcohol) films. *J Appl Polym Sci* 2004;91:2407–15. doi:10.1002/app.13400.
- [6] Lyoo W, Yeum J, Ghim H, Park J, Lee S, Kim J, et al. Effect of the molecular weight of poly(vinyl alcohol) on the water stability of a syndiotactic poly(vinyl alcohol)/iodine complex film. *Colloid Polym Sci* 2003;281:416–22. doi:10.1007/s00396-002-0788-7.
- [7] Broer DJ, Boven J, Mol GN, Challa G. In-situ photopolymerization of oriented liquid-crystalline acrylates, 3. Oriented polymer networks from a mesogenic diacrylate. *Makromol Chem* 1989;190:2255–68. doi:10.1002/macp.1989.021900926.
- [8] Peeters E, Lub J, Steenbakkens JAM, Broer DJ. High-Contrast Thin-Film Polarizers by Photo-Crosslinking of Smectic Guest-Host Systems. *Adv Mater* 2006;18:2412–7. doi:10.1002/adma.200600355.
- [9] Van der Zande BMI, Roosendaal SJ, Doornkamp C, Steenbakkens J, Lub J. Synthesis, Properties, and Photopolymerization of Liquid-Crystalline Oxetanes: Application in Transflective Liquid-Crystal Displays. *Adv Funct Mater* 2006;16:791–8. doi:10.1002/adfm.200500359.
- [10] Broer DJ, Lub J, Mol GN. Wide-band reflective polarizers from cholesteric polymer networks with a pitch gradient. *Nature* 1995;378:467–9. doi:10.1038/378467a0.
- [11] Van de Witte P, Haaren J van, Tuijtelars J, Stallinga S, Lub J. Preparation of Retarders with a Tilted Optic Axis. *Jpn J Appl Phys* 1999;38:748–54. doi:10.1143/JJAP.38.748.
- [12] Lub J, van de Witte P, Doornkamp C, Vogels JP, Wegh RT. Stable Photopatterned Cholesteric Layers Made by Photoisomerization and Subsequent Photopolymerization for Use as Color Filters in Liquid-Crystal Displays. *Adv Mater* 2003;15:1420–5. doi:10.1002/adma.200305125.
- [13] Ivashchenko AV. *Dichroic dyes for liquid crystal displays*. Boca Raton: CRC Press; 1994.
- [14] Heilmeyer GH, Zanoni LA. Guest-host interactions in nematic liquid crystals. A new electro-optic effect. *Appl Phys Lett* 1968;13:91–2. doi:10.1063/1.1652529.
- [15] White DL, Taylor GN. New absorptive mode reflective liquid-crystal display device. *J Appl Phys* 1974;45:4718–23. doi:10.1063/1.1663124.
- [16] Chigrinov VG. *Liquid crystal devices: physics and applications*. Boston: Artech House; 1999.
- [17] Iwanaga H, Taira K, Nakai Y. Color Design and Adjustment of Dichroic Dyes for Reflective Three-Layered Guest-Host Liquid Crystal Displays. *Mol Cryst Liq Cryst* 2005;443:105–16. doi:10.1080/15421400500247326.

- [18] Iwanaga H. Development of Highly Soluble Anthraquinone Dichroic Dyes and Their Application to Three-Layer Guest-Host Liquid Crystal Displays. *Materials* 2009;2:1636–61. doi:10.3390/ma2041636.
- [19] Kitson S, Geisow A, Rudin J, Taphouse T. Bright color reflective displays with interlayer reflectors. *Opt Express* 2011;19:15404. doi:10.1364/OE.19.015404.
- [20] Zhang X, Gorohmaru H, Kadowaki M, Kobayashi T, Ishi-i T, Thiemann T, et al. Benzo-2,1,3-thiadiazole-based, highly dichroic fluorescent dyes for fluorescent host-guest liquid crystal displays. *J Mater Chem* 2004;14:1901. doi:10.1039/b402645d.
- [21] Taheri B, Kosa T, Bodnar V, Sukhomlinova L, Su L, Martincic C, et al. Guest-host liquid crystal devices for adaptive window application. In: Chien L-C, editor., 2010, p. 76180W – 76180W – 10. doi:10.1117/12.848297.
- [22] Piñol R, Lub J, García MP, Peeters E, Serrano JL, Broer D, et al. Synthesis, Properties, and Polymerization of New Liquid Crystalline Monomers for Highly Ordered Guest-Host Systems. *Chem Mater* 2008;20:6076–86. doi:10.1021/cm801133b.
- [23] Matsunaga D, Tamaki T, Akiyama H, Ichimura K. Photofabrication of Micro-Patterned Polarizing Elements for Stereoscopic Displays. *Adv Mater* 2002;14:1477–80. doi:10.1002/1521-4095(20021016).
- [24] Lawrentz U, Grahn W, Lukaszuk K, Klein C, Wortmann R, Feldner A, et al. Donor-Acceptor Oligoenes with a Locked all-trans Conformation: Synthesis and Linear and Nonlinear Optical Properties. *Chem - Eur J* 2002;8:1573–90. doi:10.1002/1521-3765(20020402).
- [25] Zitzler-Kunkel A, Lenze MR, Kronenberg NM, Krause A-M, Stolte M, Meerholz K, et al. NIR-Absorbing Merocyanine Dyes for BHJ Solar Cells. *Chem Mater* 2014;26:4856–66. doi:10.1021/cm502302s.
- [26] Véron AC, Zhang H, Linden A, Nüesch F, Heier J, Hany R, et al. NIR-Absorbing Heptamethine Dyes with Tailor-Made Counterions for Application in Light to Energy Conversion. *Org Lett* 2014. doi:10.1021/ol4034385.
- [27] Chen L, Wu J, Schmuck C, Tian H. A switchable peptide sensor for real-time lysosomal tracking. *Chem Commun* 2014;50:6443. doi:10.1039/c4cc00670d.
- [28] Nandi LG, Nicoletti CR, Belletini IC, Machado VG. Optical Chemosensor for the Detection of Cyanide in Water Based On Ethyl(hydroxyethyl)cellulose Functionalized with Brooker's Merocyanine. *Anal Chem* 2014;86:4653–6. doi:10.1021/ac501233x.
- [29] Mustroph H, Reiner K, Senns B, Mistol J, Ernst S, Keil D, et al. The Effects of Substituents and Solvents on the Ground-State π -Electronic Structure and Electronic Absorption Spectra of a Series of Model Merocyanine Dyes and Their Theoretical Interpretation. *Chem - Eur J* 2012;18:8140–9. doi:10.1002/chem.201101830.
- [30] Mishra A, Behera RK, Behera PK, Mishra BK, Behera GB. Cyanines during the 1990s: A Review. *Chem Rev* 2000;100:1973–2012. doi:10.1021/cr990402t.
- [31] Panigrahi M, Dash S, Patel S, Mishra BK. Syntheses of cyanines: a review. *Tetrahedron* 2012;68:781–805. doi:10.1016/j.tet.2011.10.069.
- [32] Kreß KC, Fischer T, Stumpe J, Frey W, Raith M, Beiraghi O, et al. Influence of Chromophore Length and Acceptor Groups on the Optical Properties of Rigidified Merocyanine Dyes. *ChemPlusChem* 2014;79:223–32. doi:10.1002/cplu.201300308.
- [33] V. Percec. Amphiphilic dendritic dipeptides and their self-assembly into helical pores. US Patent 20060088499, 2006.
- [34] Balamurugan S, Kannan P, Chuang MT, Wu SL. Antiferroelectric Bent-Core Liquid Crystals for Molecular Switching Applications. *Ind Eng Chem Res* 2010;49:7121–8. doi:10.1021/ie100019p.
- [35] Liu J, Yang P. Optical behaviour of photoimageable cholesteric liquid crystal cells with various novel chiral compounds. *Liq Cryst* 2005;32:539–51. doi:10.1080/02678290500117654.

- [36] Gassman PG, Macomber DW, Willging SM. Isolation and characterization of reactive intermediates and active catalysts in homogeneous catalysis. *J Am Chem Soc* 1985;107:2380–8. doi:10.1021/ja00294a031.
- [37] Shi Y, Zhang J, Stein PD, Shi M, O'Connor SP, Bisaha SN, et al. Ketene aminal-based lactam derivatives as a novel class of orally active FXa inhibitors. *Bioorg Med Chem Lett* 2005;15:5453–8. doi:10.1016/j.bmcl.2005.08.107.
- [38] Lawrentz U. Synthesen und Eigenschaften planar fixierter und oligomerer Polymethinfarbstoffe. Technische Universität Braunschweig; 2002.
- [39] Meerwein H, Florian W, Schön N, Stopp G. Über Säureamidacetale, Harnstoffacetale und Lactamacetale. *Justus Liebigs Ann Chem* 1961;641:1–39. doi:10.1002/jlac.19616410102.
- [40] Mangalum A, Gilliard Jr. RJ, Hanley JM, Parker AM, Smith RC. Metal ion detection by luminescent 1,3-bis(dimethylaminomethyl) phenyl receptor-modified chromophores and cruciforms. *Org Biomol Chem* 2010;8:5620–7. doi:10.1039/c0ob00156b.
- [41] Chen W-H, Chuang W-T, Jeng U-S, Sheu H-S, Lin H-C. New SmCG Phases in a Hydrogen-Bonded Bent-Core Liquid Crystal Featuring a Branched Siloxane Terminal Group. *J Am Chem Soc* 2011;133:15674–85. doi:10.1021/ja205550b.
- [42] Parker CO. Oxygen alkylation of negatively substituted esters. *J Am Chem Soc* 1956;78:4944–7.
- [43] Li J, van Belkum MJ, Vederas JC. Functional characterization of recombinant hyoscyamine 6 β -hydroxylase from *Atropa belladonna*. *Bioorg Med Chem* 2012;20:4356–63. doi:10.1016/j.bmc.2012.05.042.
- [44] Greenhill JV. Reaction of *t*-butylamine with cyclohexane-1,3-dione. *J Chem Soc C Org* 1970:1002–4. doi:10.1039/j39700001002.
- [45] Suhan ND, Loeb SJ, Eichhorn SH. Mesomorphic [2]Rotaxanes: Sheltering Ionic Cores with Interlocking Components. *J Am Chem Soc* 2013;135:400–8. doi:10.1021/ja309558p.
- [46] Marcos M, Giménez R, Serrano JL, Donnio B, Heinrich B, Guillon D. Dendromesogens: liquid crystal organizations of poly(amidoamine) dendrimers versus starburst structures. *Chem Weinh Bergstr Ger* 2001;7:1006–13.
- [47] Doolittle AK. Studies in Newtonian Flow. II. The Dependence of the Viscosity of Liquids on Free-Space. *J Appl Phys* 1951;22:1471–5. doi:10.1063/1.1699894.
- [48] Gavezzotti A. Molecular aggregation: structure analysis and molecular simulation of crystals and liquids. Oxford ; New York: Oxford University Press; 2007.
- [49] Demus D, Goodby JWG, Gray GW. Handbook of liquid crystals. Vol. 2A, Low molecular weight liquid crystals I. Weinheim; New York; Chichester: Wiley-VCH; 1998.
- [50] Bruce DW, Dunmur DA, Hunt SE, Maitlis PM, Orr R. Linear dichroism of mesomorphic transition-metal complexes of alkoxydithiobenzoates. *J Mater Chem* 1991;1:857. doi:10.1039/jm9910100857.
- [51] Korte EH. Influence of the Order Parameter *D* on the Linear Dichroism of Nematic Liquid Crystals. *Mol Cryst Liq Cryst* 1983;100:127–35. doi:10.1080/00268948308073726.
- [52] Kelly SM. Flat panel displays: advanced organic materials. Cambridge: Royal Society of Chemistry; 2000.
- [53] Rutgers GAW. Standards for Photometry. *Appl Opt* 1971;10:2595–9. doi:10.1364/AO.10.002595.
- [54] Franck B, Schneider U. PHOTOOXIDATION PRODUCTS OF MEROCYANINE 540 FORMED UNDER PREAMBINATION CONDITIONS FOR TUMOR THERAPY. *Photochem Photobiol* 1992;56:271–6. doi:10.1111/j.1751-1097.1992.tb02157.x.
- [55] Abdel-Kader MH, Steiner U. A molecular reaction cycle with a solvatochromic merocyanine dye: an experiment in photochemistry, kinetics, and catalysis. *J Chem Educ* 1983;60:160. doi:10.1021/ed060p160.

- [56] Kalyanaraman B, Feix JB, Sieber F, Thomas JP, Girotti AW. Photodynamic action of merocyanine 540 on artificial and natural cell membranes: involvement of singlet molecular oxygen. *Proc Natl Acad Sci U S A* 1987;84:2999–3003.
- [57] Pervaiz S. Reactive oxygen-dependent production of novel photochemotherapeutic agents. *FASEB J* 2001;15:612–7. doi:10.1096/fj.00-0555rev.
- [58] Sobbi AK, Wöhrle D, Schlettwein D. Photochemical stability of various porphyrins in solution and as thin film electrodes. *J Chem Soc Perkin Trans 2* 1993:481. doi:10.1039/p29930000481.

ACCEPTED MANUSCRIPT

Figure 1 Optimized geometry of *E*-**MC 4a**.

Table 1 Calculated aspect ratios basing on the DFT calculation (B3LYP 3-21G*) of the merocyanines.

$${}^a L_{chain} = V_{chain}/\pi(0.5W_{chain})^2, {}^b \text{aspect ratio } AR = (L_{chain} + L_{chore})/W_{chore}.$$

Table 2 Absorption maxima, dichroic ratio and averaged aspect ratio of the investigated merocyanines.

Figure 2 Linearly-polarised absorption spectra of **MC 2** and **MC 6** in LC cells parallel and perpendicular to the orientation

Figure 3 Observed dichroic ratio of **MC 1**, **MC 2**, **MC 3** in a LC cell as a function the wavelength of their absorption maxima (a) and on their calculated aspect ratio (b, Table 1).

Figure 4 Absorbance and emission spectra of **MC 3** in a RMM matrix upon parallel and perpendicular excitation.

Figure 5 Observed dichroic ratio of merocyanines in a RMM34 matrix and their corresponding absorption maxima.

Figure 6 UV/Vis-spectra of **MC 3** in CH₃CN upon irradiation with a xenon lamp as a function of time.

Figure 7 Normalized absorbance at λ_{max} in CH₃CN as a function of the corrected light dose.

Figure 8 Normalized absorbance at 593 nm of **MC 3**.

Figure 9 UV/Vis-spectra of **MC 2** in a LC matrix upon irradiation with a xenon lamp as a function of time.

Figure 10 Normalized absorbance at λ_{max} in a LC matrix as a function of the irradiation time.

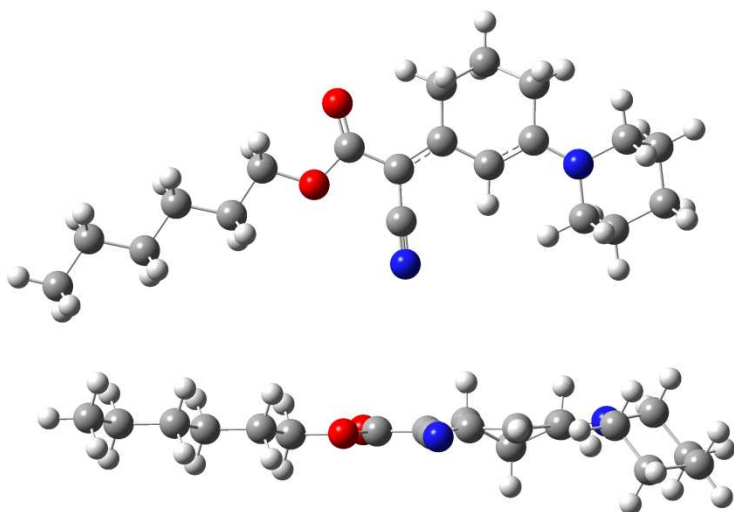
Figure 11 Emission intensity of **MC 3** in a RMM matrix as a function of time upon excitation at 590 nm.

Table 1 Calculated aspect ratios basing on the DFT calculation (B3LYP 3-21G*) of the merocyanines.
^a $L_{chain} = V_{chain}/\pi(0.5W_{chain})^2$, ^b aspect ratio $AR = (L_{chain} + L_{chore})/W_{chore}$.

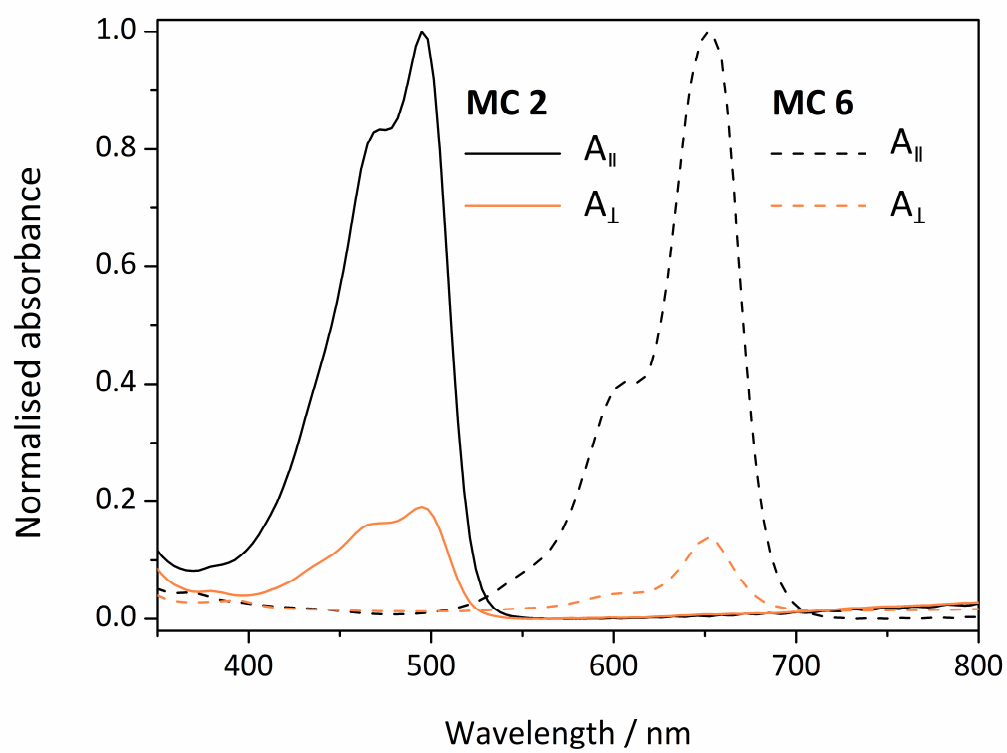
	isomer	$W_{core} / \text{\AA}$	$L_{core} / \text{\AA}$	$L_{chain}^a / \text{\AA}$	$AR_{\phi}^b / \text{\AA}$	Fraction of E/Z isomers in the mixture	$AR_{\phi} / \text{\AA}$
MC 1	E	4.95	9.94	8.6	2.53	0.29	
	Z	4.95	10.38	8.5	1.96	0.71	2.1
MC 2	E	4.96	12.86	8.5	2.64	0.55	
	Z	4.97	13.33	8.5	2.18	0.45	2.4
MC 3	E	4.96	15.04	8.5	2.76	0.46	
	Z	4.97	14.79	8.5	2.29	0.54	2.6
MC 4a	E	4.95	9.94	18.5	5.75	0.29	
	Z	4.95	10.38	18.5	5.82	0.71	5.8
MC 4b	E	4.95	9.94	24.1	6.89	0.29	
	Z	4.95	10.38	24.1	6.96	0.71	6.9
MC 4c	E	4.95	9.94	29.8	8.03	0.29	
	Z	4.95	10.38	29.7	8.10	0.71	8.1
MC 5	-	4.97	14.85	-	1.97		2.0
MC 6	-	4.94	17.80	-	1.89		1.9

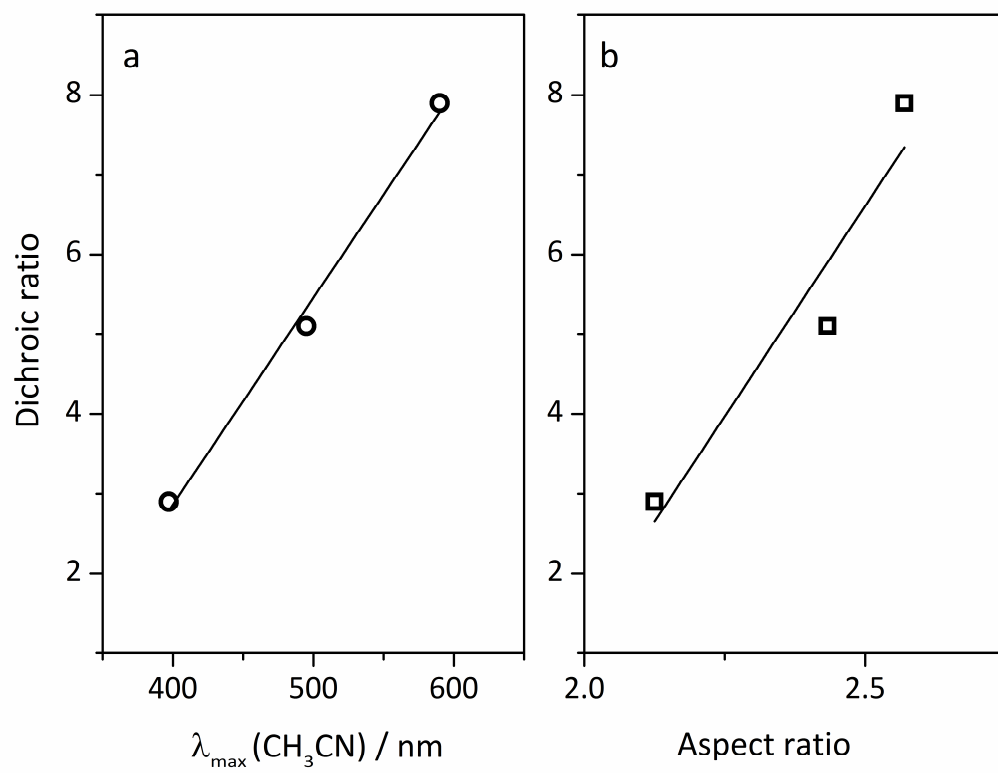
Table 2 Absorption maxima, dichroic ratio and averaged aspect ratio of the investigated merocyanines.

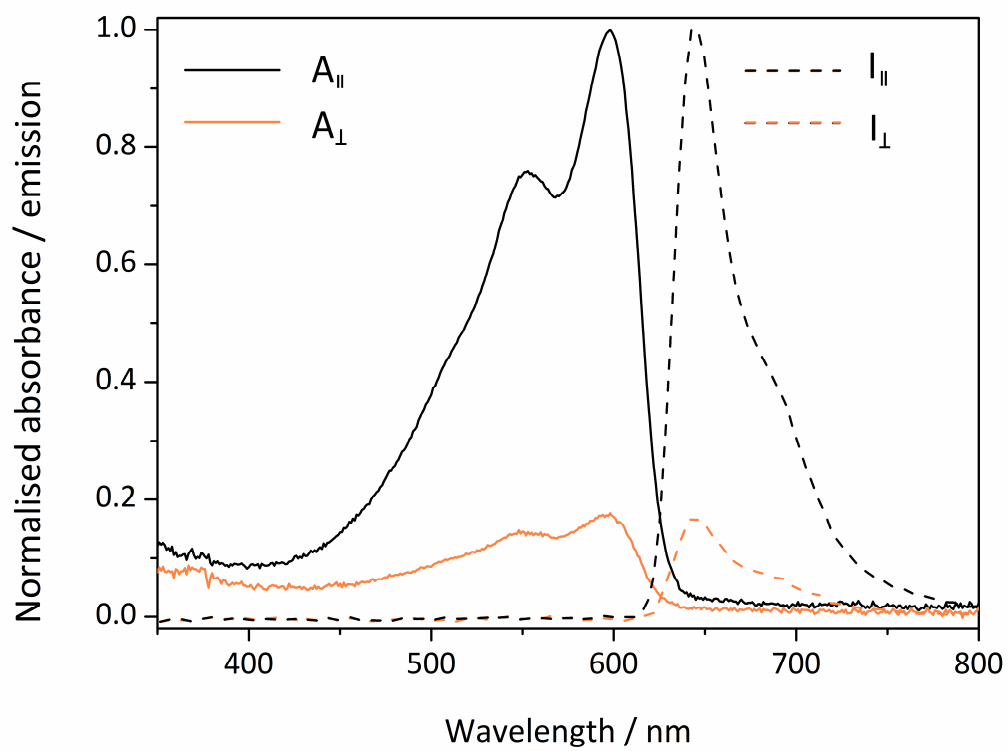
	MC 1	MC 2	MC 3	MC 4a	MC 4b	MC 4c	MC 5	MC 6
$\lambda_{max} (\text{CH}_3\text{CN}) / \text{nm}$	397	495	590	398	398	398	586	628
$AR_{\phi} / \text{\AA}$	2.1	2.4	2.6	5.8	6.9	8.1	2.0	1.9
<i>DR</i>	2.9	5.1	7.9	2.5	2.5	2.5	--	7.2

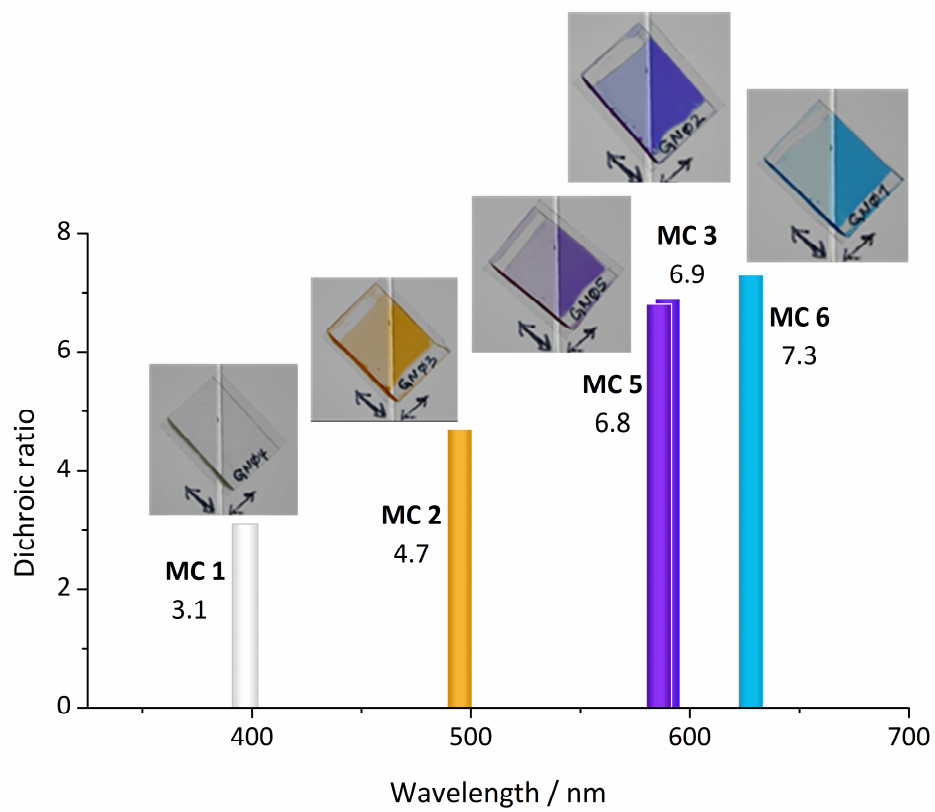


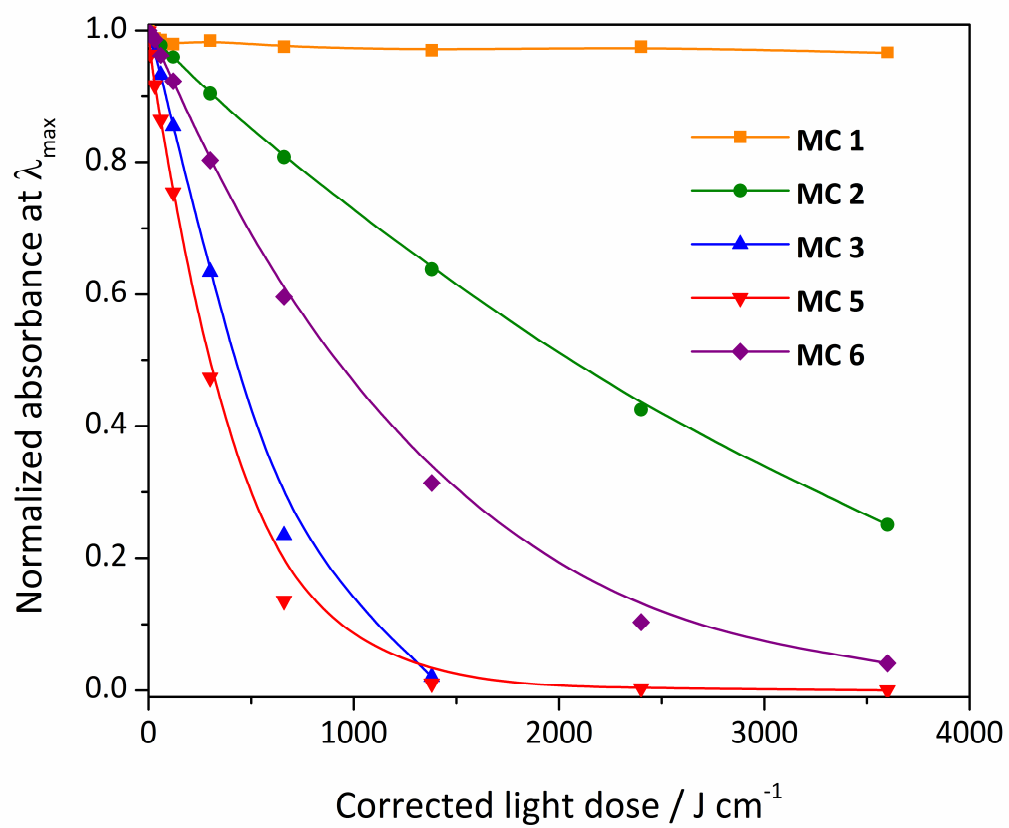
ACCEPTED MANUSCRIPT

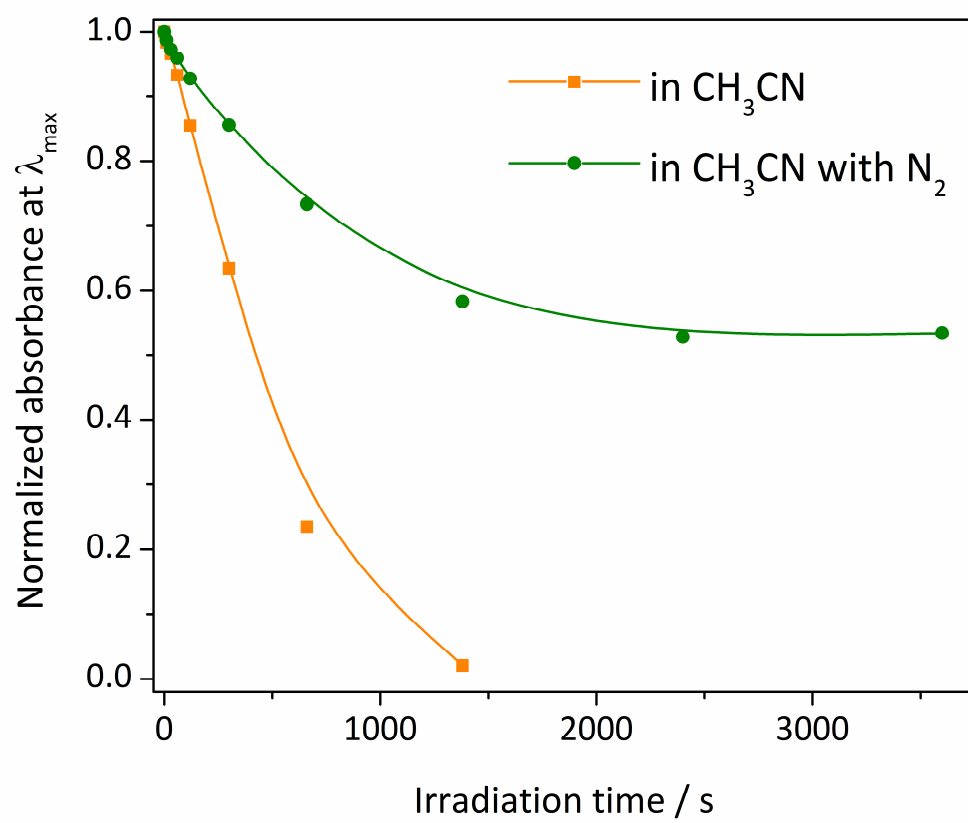


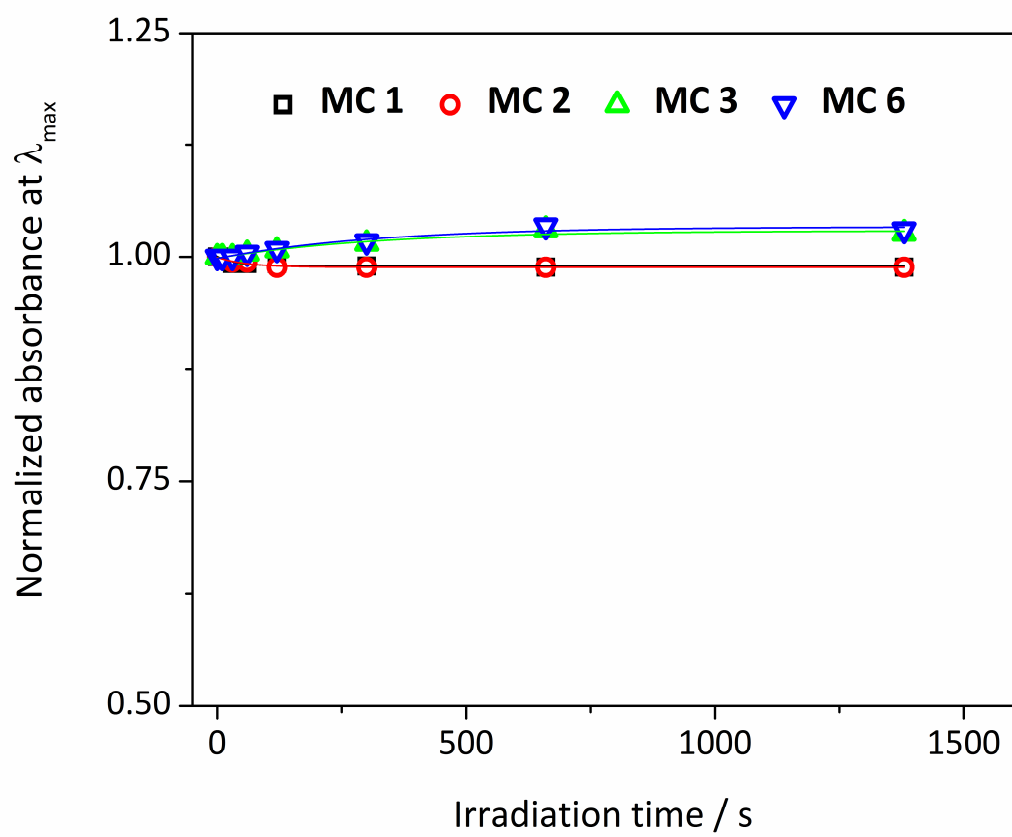




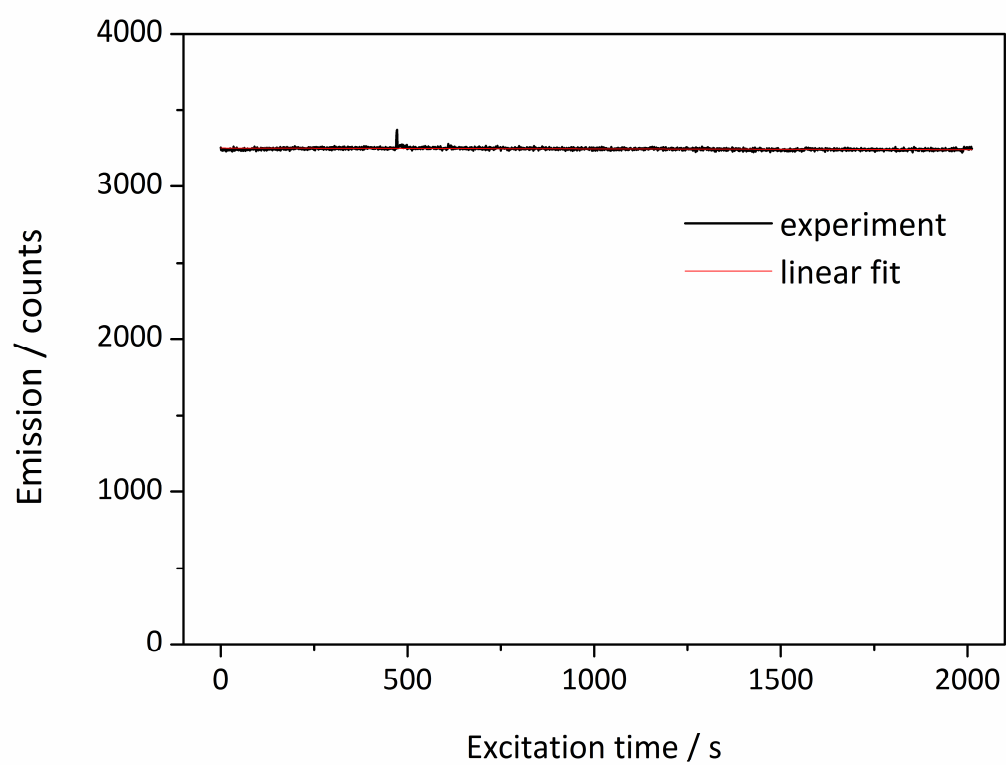








ACCEPTED MANUSCRIPT



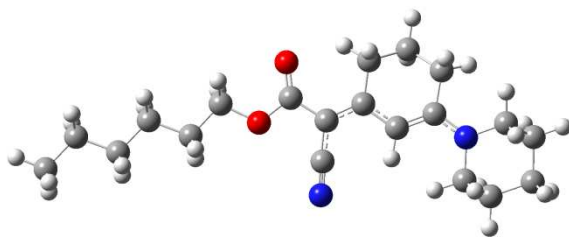
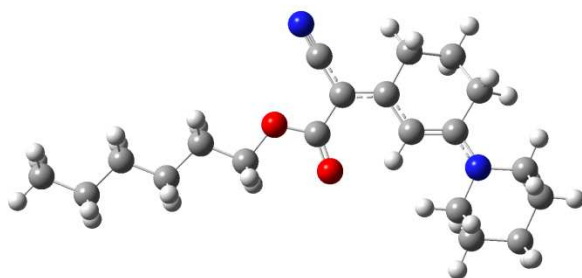
Supporting Information

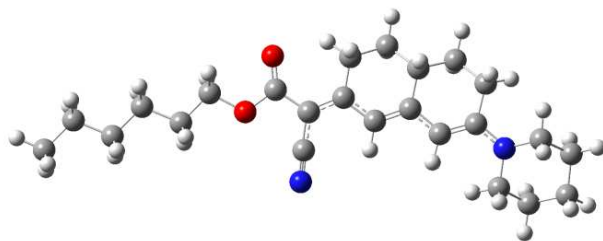
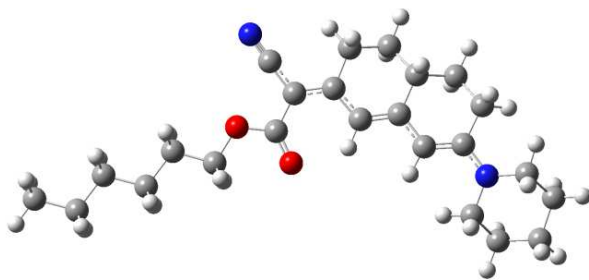
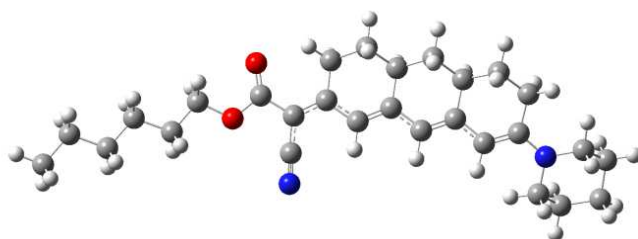
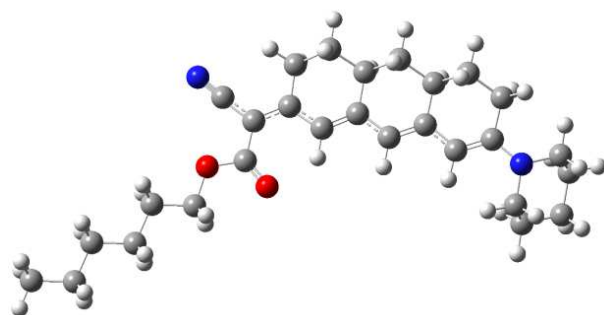
Rigidified Merocyanine Dyes with Different Aspect Ratios:

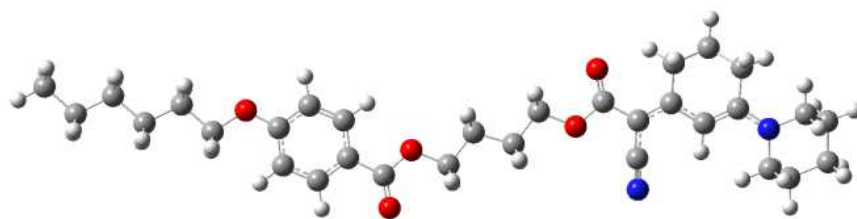
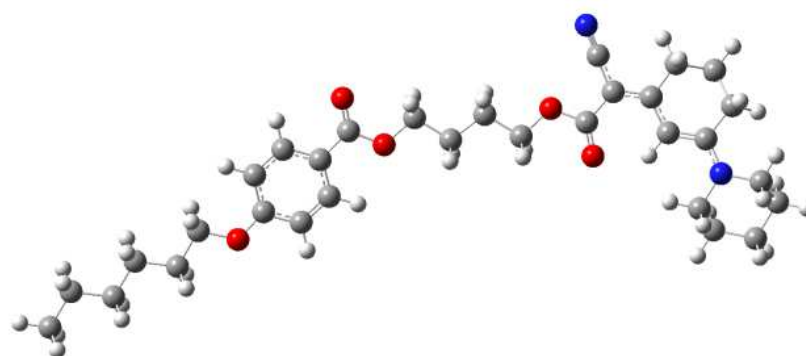
Dichroism and Photostability

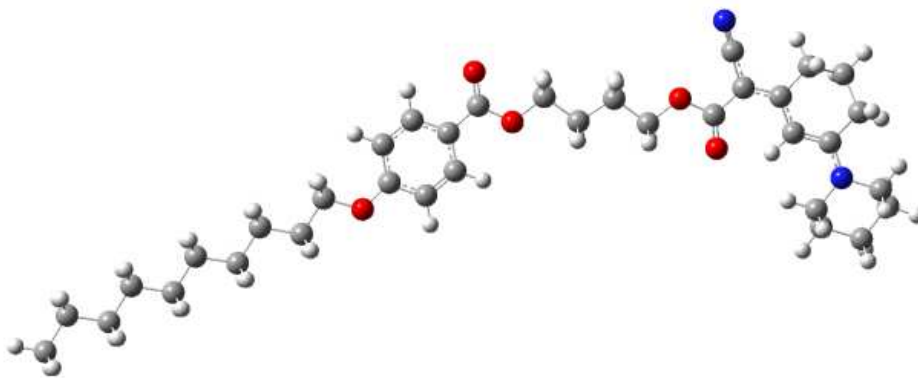
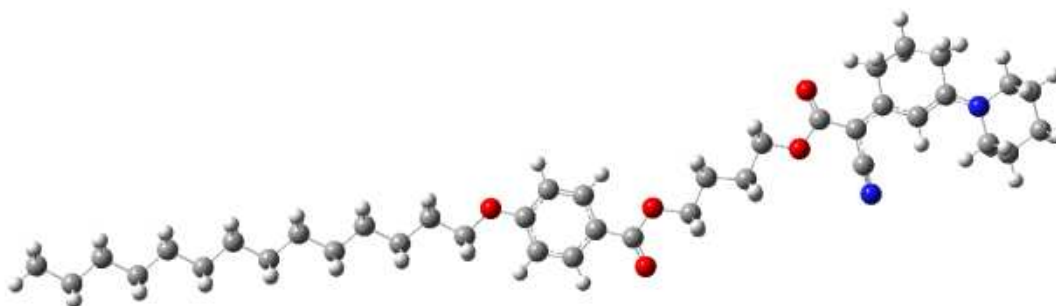
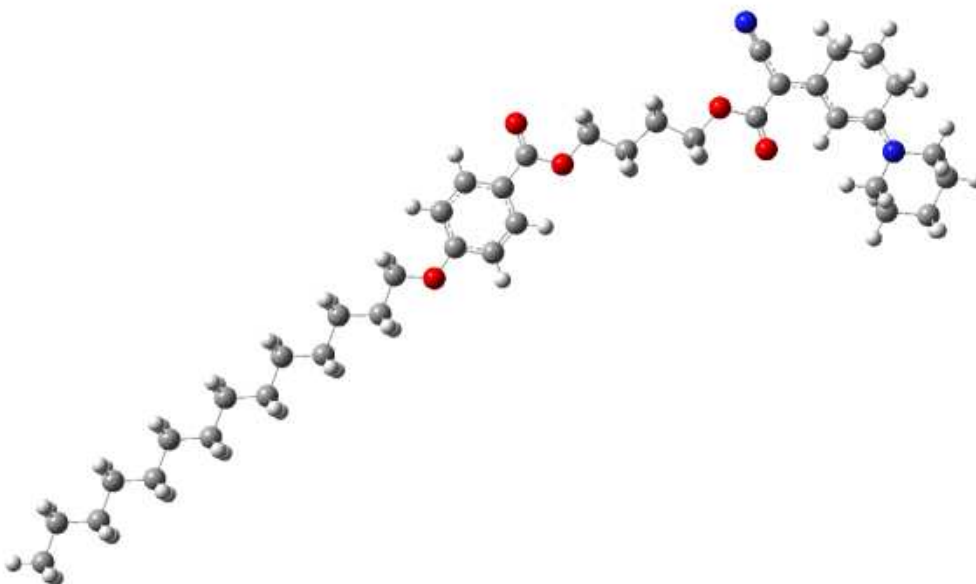
Katharina Christina Kreß,^a Korinna Bader,^a Joachim Stumpe,^b S. Holger Eichhorn^cSabine Laschat^{a*} and Thomas Fischer^b

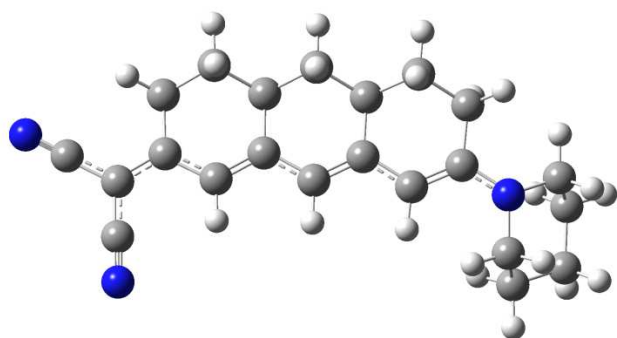
1. Structures determined by DFT calculations (B3LYP 3-21G*)

*E*-MC 1*Z*-MC 1

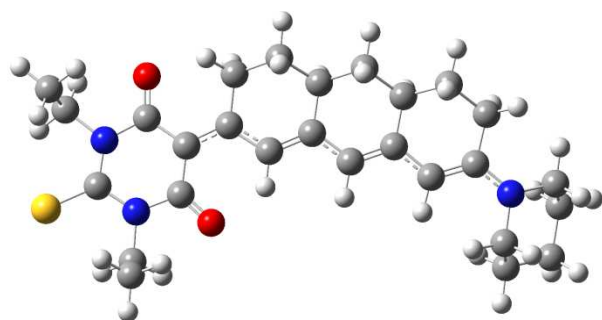
**E-MC 2****Z-MC 2****E-MC 3****Z-MC 3**

*E*-MC 4a*Z*-MC 4a*E*-MC 4b

**Z-MC 4b****E-MC 4c****Z-MC 4c**



MC 5



MC 6

2. Linearly-polarised absorption spectra

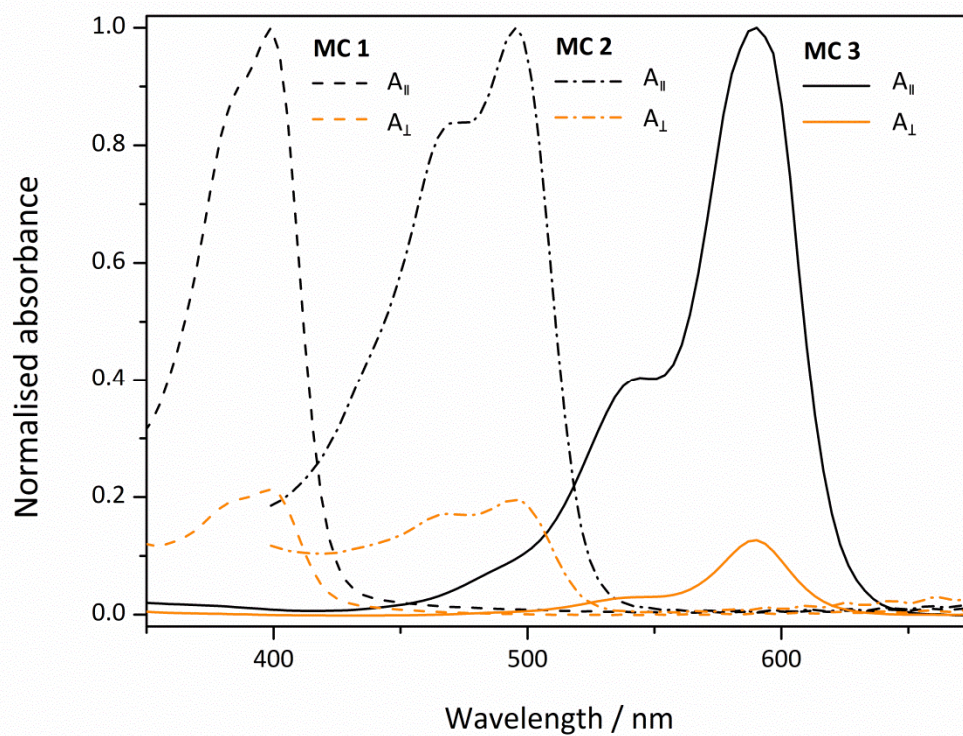


Figure 1 Linearly-polarised absorption spectra of **MC 1**, **MC 2** and **MC 3** in LC cells parallel and perpendicular to the orientation.

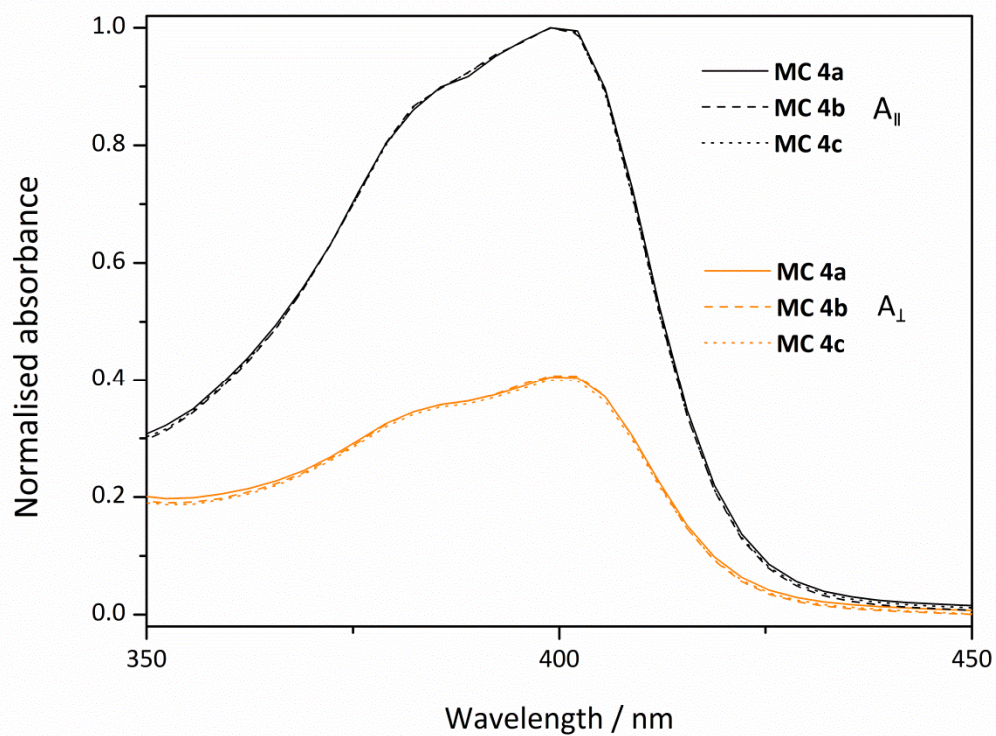


Figure 2 Linearly-polarised absorption spectra of **MC 4a**, **MC 4b** and **MC 4c** in LC cells parallel and perpendicular to the orientation.